AIMS Mathematics, 10(7): 15131–15164.
DOI: 10.3934/math.2025679
Received: 06 May 2025
Revised: 25 June 2025
Accepted: 26 June 2025
Published: 01 July 2025

https://www.aimspress.com/journal/Math

Research article

Reliability analysis for independent Nadarajah–Haghighi competing risks model employing improved adaptive progressively censored data

Refah Alotaibi[1,*], **Mazen Nassar**[2,3] **and Ahmed Elshahhat**[4]

[1] Department of Mathematical Sciences, College of Science, Princess Nourah bint Abdulrahman University, P.O. Box 84428, Riyadh 11671, Saudi Arabia

[2] Department of Statistics, Faculty of Science, King Abdulaziz University, Jeddah 21589, Saudi Arabia

[3] Department of Statistics, Faculty of Commerce, Zagazig University, Zagazig, Egypt

[4] Faculty of Technology and Development, Zagazig University, Zagazig 44519, Egypt

* **Correspondence:** Email: rmalotaibi@pnu.edu.sa.

Abstract: The use of competing risk frameworks for the analysis of reliability/survival data has gained popularity in recent years, primarily because traditional techniques are inadequate for effectively analyzing such data. In this study, we examined the independent competing risks model with lifetimes of units distributed according to the Nadarajah–Haghighi distribution. Our focus was on estimating the unknown parameters, as well as the reliability and failure rate functions, using both frequentist and Bayesian estimation methods under an improved adaptive progressive Type-II censoring mechanism. The frequentist estimation involved deriving point estimators and approximate confidence intervals using the asymptotic properties of classical estimators. Bayes estimators were obtained through symmetric squared loss and the Metropolis-Hastings algorithm, which generated samples from the joint posterior distribution. Additionally, the highest posterior density credible intervals were calculated. Given the complex nature of the acquired estimators, we conducted a comprehensive simulation study to numerically compare the performance of the proposed estimates across various experimental scenarios. To empirically validate the proposed inferential framework, we analyzed two real-world competing risk datasets, highlighting the effectiveness of the applied techniques in reliability data analysis.

Keywords: Nadarajah–Haghighi; survival analysis competing risks; improved adaptive progressive censoring; Bayesian; electrical appliances; multiple myeloma
Mathematics Subject Classification: 62F10, 62F15, 62N01, 62N05

1. Introduction

In numerous empirical research domains, such as medical and engineering fields, the failure of experimental units may be attributed to multiple underlying factors, for example, various triggers for cancer relapse. In lifetime experiments, researchers typically concentrate on analyzing specific failure modes when multiple risk factors exist. This methodological challenge is commonly referred to as the competing risks framework in scholarly works. When analyzing competing risk datasets, the information comprises both the time-to-event for failed specimens and a categorical marker denoting the failure cause. Our methodology adopts the latent failure time paradigm, initially proposed by Cox [1], which operates under the assumption of independence between potential failure times associated with each distinct risk. Within existing research on competing risk analysis, numerous studies utilize various lifetime probability distributions to model empirical datasets. A primary emphasis in these works has been on parametric inference methodologies, while limited attention has been directed toward examining reliability metrics or reliability measures. For instance, see Cramer and Schmiedt [2], Ahmed et al. [3], Abushal et al. [4], Almuqrin et al. [5], Tian et al. [6], and Alotaibi et al. [7], among others.

Researchers examining the field of statistical distribution theory will observe that numerous novel probability models have been recently developed through either composite formulations of existing distributions or by introducing additional parameters to classical models. Recent contributions in this area include the works of Han et al. [8], Haddari et al. [9], Kouadriaand Zeghdoudi [10], and Kumar et al. [11]. This trend aims to enhance distributional flexibility for improved empirical adaptability. However, many contemporary distributions feature three or more parameters, creating implementation challenges in reliability studies and lifetime experiments. This complexity becomes particularly pronounced in competing risk frameworks, where parameter duplication occurs across failure modes. Among notable exceptions, the Nadarajah–Haghighi (NH) distribution stands out as a flexible model proposed by Nadarajah and Haghighi [12], balancing mathematical tractability with analytical utility. The NH distribution is characterized by a scale parameter and a shape parameter. Nadarajah and Haghighi [12] demonstrated that its probability density function (PDF) can exhibit decreasing or unimodal forms, while the failure rate function (FRF) exhibits flexible failure patterns including increasing, decreasing, or constant forms, similar to those of Weibull, gamma, and exponentiated exponential models. Multiple studies have addressed the challenges in estimating both parameters and related reliability metrics for the NH distribution, including but not limited to the work of Wu and Gui [13], Dey et al. [14], Elbatal et al. [15], Almarashi et al. [16], Abushal [17], and Abd Elwahab [18]. The subsequent section will detail structural properties of the independent NH competing risks framework, encompassing its PDF, cumulative distribution function (CDF), reliability function (RF), and FRF.

In life testing studies and reliability analysis involving multiple failure causes, researchers often terminate tests before all units fail. This is done for practical reasons, such as reducing time and cost or because some items have exceptionally long lifespan. When tests end early, only partial failure data is collected. In statistical literature, such data is referred to as censored data. Researchers have developed various censored data collection methods, known as censoring plans, each defined by a specific condition to terminate the test. Common approaches include Type I censoring, where testing stops after a fixed time, Type II censoring, which ends when a predetermined number of failures occur,

and hybrid methods that combine both time-based and count-based criteria; see Balakrishnan and Kundu [19] for more details. A more flexible approach known as progressive Type-II censoring (PTIIC) enables researchers to eliminate functioning items during testing at multiple stages, rather than solely at the final endpoint. This method generalizes traditional censoring by permitting the gradual removal of unfailed units throughout the experiment. This censoring mechanism has been thoroughly investigated in statistical literature, see for example Balakrishnan et al. [20], Rastogi and Tripathi [21], Abo-Kasem et al. [22], and Hasaballah et al. [23].

A more adaptable censoring strategy developed by Ng et al. [24], called the adaptive PTIIC (APTIIC), generalizes earlier methods by incorporating PTIIC, Type-II censoring, and complete sampling as special cases. The APTIIC guarantees a fixed number of failures by test completion while enabling experimenters to halt the removal of functional units once a predefined time threshold is reached. This hybrid approach provides flexibility in experimental design and strengthens the practical utility of censored data analysis. Some notable studies in this area include Sobhi and Soliman [25], Panahi and Moradi [26], and Dutta et al. [27]. Ng et al. [24] highlighted that the APTIIC strategy is most effective when there is no strict time constraint on testing. However, for products that have high reliability, this methodology can lead to excessively lengthy experiments, which may not be feasible. To address this challenge, Yan et al. [28] suggested a new version known as the improved APTIIC (IAPTIIC) scheme. This new approach integrates concepts from PTIIC, APTIIC, and various censoring plans while ensuring that the testing concludes by a predefined time. Additionally, it maintains the total number of failures that researchers aim to observe. By effectively balancing the aspects of time and failure count, the IAPTIIC presents a more practical solution. In the subsequent section, we will clarify the framework of the IAPTIIC within the competing risks model.

Three key considerations that encourage us to complete this investigation are: (1) the operational effectiveness of the IAPTIIC framework in achieving time-bound experimental outcomes, which is particularly critical for studies involving high-reliability products; (2) the essential role of competing risks methodology in reliability analysis, particularly in contexts where multiple failure causes exist; and (3) the demonstrated flexibility of the NH distribution in modeling various failure patterns. The NH distribution was selected due to its flexibility in modeling various shapes of hazard rates, making it suitable for reliability studies with complex failure patterns. Its ability to accommodate both increasing and decreasing hazard rates enhances its applicability under different experimental conditions. Moreover, the NH distribution provided a suitable fit to the two real-world competing risks datasets analyzed in this study, as discussed later in the real data section, further justifying its use in the proposed inferential framework. Although other competitive models may yield a better fit in specific scenarios, the NH distribution was selected due to its structural simplicity and its broad recognition in the existing literature. Utilizing these factors, the primary objective of this work is to develop estimation methodologies for the parameter, RF and FRF of the NH competing risks model under IAPTIIC-censored data. This work offers several methodological and practical contributions to the field of reliability analysis. First, it introduces the NH distribution into the context of competing risks modeling under the IAPTIIC scheme, providing a more flexible and time-efficient approach to reliability testing. Second, it develops both frequentist and Bayesian inference methods and compares the effectiveness of the proposed methods through simulation studies and real-world reliability applications, highlighting their ability to handle multiple causes of failure under constrained experimental conditions.

The detailed aims of this work are systematically structured as follows:

(1) Establish the statistical framework for the NH competing risks model, including the derivation of the RF and FRF, as well as formalizing the joint likelihood under observed IAPTIIC data.
(2) Develop frequentist inference procedures to estimate the model parameters, RF, and FRF. These procedures will encompass both maximum likelihood estimates (MLEs) and associated approximate confidence intervals (ACIs).
(3) Implement Bayesian inference paradigms employing informative priors. Posterior estimates will be computed under squared error loss, with posterior samples generated using Metropolis-Hastings (MH) algorithms.
(4) Conduct comprehensive Monte Carlo simulations to evaluate the performance of the acquired point and interval estimates across varying sample sizes, progressive censoring designs, and time thresholds.
(5) Execute empirical validation through two reliability applications, demonstrating the practical implementation of the proposed estimators besides assessing model adequacy.

This paper is structured as follows: Section 2 introduces the NH competing risks model under the IAPTIIC scheme. Section 3 derives the MLEs and ACIs for model parameters, RF, and FRF. Section 4 develops Bayesian estimation procedures using squared error loss and constructs highest posterior density (HPD) credible intervals. Section 5 outlines the simulation design and presents numerical results. Section 6 applies the proposed methods to real-world data. Finally, Section 7 concludes the paper with key findings.

2. Model description and notation

This study concentrates on analyzing reliability data characterized by two independent failure mechanisms, and the methodological framework can be extended to encompass multiple competing failure modes. Consider an experiment involving n units with lifetimes determined by independent and identically distributed (iid) random variables $Y_1, \ldots, Y_n$. Each observed failure mechanism arises from one of two mutually exclusive causes. Formally, for the i-th unit, we define:

$$Y_i = \min(Y_{1i}, Y_{2i}), \ i = 1, \ldots, n,$$

where Y_{ci}, with $c \in \{1, 2\}$, corresponds to the latent failure time of the i-th experimental unit subjected to the c-th competing risk factor. Additionally, the latent failure durations Y_{1i} and Y_{2i} $(i = 1, \ldots, n)$ are presumed statistically independent. For each observed failure event, we record both the lifetime Y_i and a categorical indicator $\delta_i \in \{1, 2\}$, where $\delta_i = \arg\min_{c\in\{1,2\}} Y_{ci}$. Here, $\delta_i = 1$ signifies failure attribution to the first risk factor, and $\delta_i = 2$ identifies termination due to the second risk factor. This failure-mode labeling enables systematic categorization of experimental outcomes. Assuming each Y_{ci} $(c = 1, 2;$ $i = 1, \ldots, n)$ follows the NH distribution parameterized by scale parameter λ_c and shape parameter $\sigma_c, c = 1, 2$, denoted $Y_{ci} \sim \text{NH}(\lambda_c, \sigma_c)$, then the PDF and CDF are, respectively, given by

$$f_c(y; \lambda_c, \sigma_c) = \lambda_c \sigma_c [\omega(y; \lambda_c)]^{\sigma_c - 1} e^{1-[\omega(y;\lambda_c)]^{\sigma_c}}, y > 0, \ \lambda_c, \sigma_c > 0, \tag{2.1}$$

and

$$F_c(y; \lambda_c, \sigma_c) = 1 - e^{1-[\omega(y;\lambda_c)]^{\sigma_c}}, \tag{2.2}$$

where $\omega(y;\lambda_c) = (1+\lambda_c y)$.

On the other hand, the RF of Y_i at any distinct time, say t, can be obtained using the relation $S(t;\boldsymbol{\Theta}) = P(Y_1 > t)P(Y_2 > t)$, where $S(t;\boldsymbol{\Theta})$ denotes to the RF and $\boldsymbol{\Theta} = (\lambda_1, \lambda_2, \sigma_1, \sigma_2)^\top$ represents the full parameter vector, and the CDF in (2.2) through the independence assumption is

$$S(t;\boldsymbol{\Theta}) = \exp\left\{2 - \sum\nolimits_{c=1}^{2} [\omega(t;\lambda_c)]^{\sigma_c}\right\}. \tag{2.3}$$

Consequently, the FRF of Y_i can be obtained using (2.3) as

$$h(t;\boldsymbol{\Theta}) = \sum\nolimits_{c=1}^{2} \lambda_c \sigma_c [\omega(y;\lambda_c)]^{\sigma_c - 1}. \tag{2.4}$$

The IAPTIIC sampling mechanism under competing risks operates as follows: Let $m < n$ denote the predetermined number of failures to observe, with $\mathbf{Q} = (Q_1, \ldots, Q_m)$ representing the prespecified removal protocol. The experimenter establishes two critical time thresholds $T_1 < T_2$. These points establish the limits of the experimental time frame: testing may continue beyond T_1 but must conclude by T_2. At each observed failure time $Y_{i:m:n}$ $(i = 1, \ldots, m)$, the experimenter removes Q_i surviving units from the remaining $Q_i = n - i - \sum_{j=1}^{i-1} Q_j$ functional items. Concurrently, the failure mode indicator $\delta_i \in \{1, 2\}$ is recorded. The experiment progresses until one of the following terminal scenarios is observed:

- **Case I (PTIIC scenario):** If $Y_{m:m:n} < T_1$, the experiment terminates at $Y_{m:m:n}$ with removal of all surviving units $Q_m = n - m - \sum_{i=1}^{m-1} Q_i$. This yields the conventional PTIIC sample.
- **Case II (APTIIC scenario):** When $Y_{d_1:m:n} < T_1 < Y_{d_1+1:m:n}$ for $d_1 < m$, an adaptive adjustment occurs:
  - Removals stopped between T_1 and $Y_{m:m:n}$ $(Q_{r_1+1} = \cdots = Q_{m-1} = 0)$
  - Experiment continues until $Y_{m:m:n}$
  - Final removal $Q_m^* = n - m - \sum_{i=1}^{d_1} Q_i$

  This generates the APTIIC sample.
- **Case III (Time-constrained scenario):** If $Y_{m:m:n} > T_2$, the study concludes at T_2 with:
  - d_2 observed failures where $Y_{d_2:m:n} \le T_2 < Y_{d_2+1:m:n}$
  - Removals stopped after T_1: $Q_{d_1+1} = \cdots = Q_{d_2} = 0$
  - Final withdrawal $Q^* = n - d_2 - \sum_{i=1}^{d_1} Q_i$

Let $\underline{\mathbf{y}}$ represent an IAPTIIC competing risks dataset collected from a continuous population with the following observed sample structure

$$\underline{\mathbf{y}} = \left\{(y_1, \delta_1, Q_1), \ldots, (y_{d_1}, \delta_{d_1}, Q_{d_1}), (y_{d_1+1}, \delta_{d_1+1}, 0), \ldots, (y_{d_2}, \delta_{d_2}, 0), (T_2, S^*)\right\},$$

where $y_i \equiv y_{i:m:n}$ simplifies notation. The corresponding likelihood function (up to proportionality) becomes

$$\begin{aligned} L(\boldsymbol{\Theta}|\underline{\mathbf{y}}) &= \left\{\prod_{i=1}^{D} \left[f_1(y_i;\lambda_1,\sigma_1)\bar{F}_2(y_i;\lambda_2,\sigma_2)\right]^{\mathbb{I}(\delta_i=1)} \left[f_2(y_i;\lambda_2,\sigma_2)\bar{F}_1(y_i;\lambda_1,\sigma_1)\right]^{\mathbb{I}(\delta_i=2)}\right\} \\ &\times \left\{\prod_{i=1}^{J} \left[\bar{F}_1(y_i;\lambda_1,\sigma_1)\bar{F}_2(y_i;\lambda_2,\sigma_2)\right]^{Q_i}\right\} \left[\bar{F}_1(\eta;\lambda_1,\sigma_1)\bar{F}_2(\eta;\lambda_2,\sigma_2)\right]^{S^*}, \end{aligned} \tag{2.5}$$

where $\bar{F}_c(\cdot) = 1 - F_c(\cdot)$, and

$$\mathbb{I}(\delta_i = c) = \begin{cases} 1 & \delta_i = c \\ 0 & \text{otherwise} \end{cases}, \quad D = \begin{cases} m & \text{Cases I/II} \\ d_2 & \text{Case III} \end{cases}, \quad J = \begin{cases} m-1 & \text{Case I} \\ d_1 & \text{Cases II/III} \end{cases},$$

$$S^* = \begin{cases} Q_m & \text{Case I} \\ Q_m^* & \text{Case II} \\ Q^* & \text{Case III} \end{cases}, \quad \eta = \begin{cases} y_m & \text{Cases I/II} \\ T_2 & \text{Case III} \end{cases}.$$

The subsequent sections develop frequentist inference methodologies and Bayesian paradigms to derive both point estimates and confidence/credible intervals for the model parameters and reliability metrics.

3. Maximum likelihood estimation

This section develops MLEs and ACIs for the NH distribution parameters $\boldsymbol{\Theta}$ and their associated reliability metrics. Under the IAPTIIC competing risks framework outlined previously, we derive these estimates using an observed sample $\underline{\mathbf{y}}$ drawn from an NH population with PDF and CDF as defined in (2.1) and (2.2), respectively. Using these functions, the joint likelihood function in (2.5) can be expressed as

$$\begin{aligned} L(\boldsymbol{\Theta}|\underline{\mathbf{y}}) &= \left[\prod_{c=1}^{2}(\lambda_c\sigma_c)^{D_c}\right]\exp\left\{\sum_{c=1}^{2}\sum_{i=1}^{D_c}(\sigma_c-1)\log[\omega(y_i;\lambda_c)] - \sum_{c=1}^{2}\sum_{i=1}^{D}[\omega(y_i;\lambda_c)]^{\sigma_c}\right. \\ &- \left.\sum_{c=1}^{2}\sum_{i=1}^{J}Q_i[\omega(y_i;\lambda_c)]^{\sigma_c} - \sum_{c=1}^{2}S^*[\omega(\eta;\lambda_c)]^{\sigma_c}\right\}, \end{aligned} \tag{3.1}$$

where $D_c = \sum_{i=1}^{D}\mathbb{I}(\delta_i = c)$ quantifies the total number of recorded failure linked to risk factor c. The log-likelihood function corresponding to (3.1), denoted by $\ell(\boldsymbol{\Theta}|\underline{\mathbf{y}})$, follows

$$\begin{aligned} \ell(\boldsymbol{\Theta}|\underline{\mathbf{y}}) &= \sum_{c=1}^{2}D_c\log(\lambda_c\sigma_c) + \sum_{c=1}^{2}\sum_{i=1}^{D_c}(\sigma_c-1)\log[\omega(y_i;\lambda_c)] - \sum_{c=1}^{2}\sum_{i=1}^{D}[\omega(y_i;\lambda_c)]^{\sigma_c} \\ &- \sum_{c=1}^{2}\sum_{i=1}^{J}Q_i[\omega(y_i;\lambda_c)]^{\sigma_c} - \sum_{c=1}^{2}S^*[\omega(\eta;\lambda_c)]^{\sigma_c}. \end{aligned} \tag{3.2}$$

The MLEs $\hat{\boldsymbol{\Theta}} = (\hat{\lambda}_1, \hat{\lambda}_2, \hat{\sigma}_1, \hat{\sigma}_2)^\top$ of the model parameters are obtained by solving the system of score equations derived from the log-likelihood function in (3.2). The normal equations are provided in Appendix A. Due to the complex nature of these equations, closed-form solutions are analytically intractable. This necessitates employing iterative numerical optimization techniques such as the Newton-Raphson (NR) algorithm to approximate the estimates. By invoking the invariance property of the MLE approach, we derive estimators for the RF as $\hat{S}(t) = S(t;\hat{\boldsymbol{\Theta}})$ and FRF as $\hat{h}(t) = h(t;\hat{\boldsymbol{\Theta}})$ at any time $t > 0$ through the substitution of the true parameters with their MLEs in (2.3) and (2.4), respectively, as

$$\hat{S}(t) = \exp\left\{2 - \sum\nolimits_{c=1}^{2}[\omega(t;\hat{\lambda}_c)]^{\hat{\sigma}_c}\right\}$$

and

$$\hat{h}(t) = \sum_{c=1}^{2} \hat{\lambda}_c \hat{\sigma}_c [\omega(y; \hat{\lambda}_c)]^{\hat{\sigma}_c - 1}.$$

The construction of confidence regions for the model parameters, and their associated RF and FRF depends on estimating their asymptotic variance-covariance matrix. While classical theory derives this through the expected Fisher information matrix $\mathcal{I}(\boldsymbol{\Theta}) = -\mathbb{E}\left[\frac{\partial^2 \ell(\boldsymbol{\Theta}|\underline{\mathbf{y}})}{\partial \boldsymbol{\Theta} \partial \boldsymbol{\Theta}^\top}\right]$, the analytical complexity of evaluating these expectations leads us to employ the observed Fisher information matrix:

$$\mathcal{I}(\hat{\boldsymbol{\Theta}}) = - \left. \frac{\partial^2 \ell(\boldsymbol{\Theta}|\underline{\mathbf{y}})}{\partial \boldsymbol{\Theta} \partial \boldsymbol{\Theta}^\top} \right|_{\boldsymbol{\Theta}=\hat{\boldsymbol{\Theta}}}.$$

Given the independence of the two competing factors, the estimated variance-covariance matrix can be simplified to

$$\begin{aligned} \mathcal{I}^{-1}(\hat{\boldsymbol{\Theta}}) &= \left[\begin{array}{cccc} -\frac{\partial^2 \ell(\boldsymbol{\Theta}|\underline{\mathbf{y}})}{\partial \lambda_1^2} & 0 & -\frac{\partial^2 \ell(\boldsymbol{\Theta}|\underline{\mathbf{y}})}{\partial \lambda_1 \partial \sigma_1} & 0 \\ & -\frac{\partial^2 \ell(\boldsymbol{\Theta}|\underline{\mathbf{y}})}{\partial \lambda_2^2} & 0 & -\frac{\partial^2 \ell(\boldsymbol{\Theta}|\underline{\mathbf{y}})}{\partial \lambda_2 \partial \sigma_2} \\ & & -\frac{\partial^2 \ell(\boldsymbol{\Theta}|\underline{\mathbf{y}})}{\partial \sigma_1^2} & 0 \\ & & & -\frac{\partial^2 \ell(\boldsymbol{\Theta}|\underline{\mathbf{y}})}{\partial \sigma_2^2} \end{array} \right]^{-1}_{\boldsymbol{\Theta}=\hat{\boldsymbol{\Theta}}} \\ &= \left[\begin{array}{cccc} \hat{V}_{11} & 0 & \hat{V}_{13} & 0 \\ & \hat{V}_{22} & 0 & \hat{V}_{24} \\ & & \hat{V}_{33} & 0 \\ & & & \hat{V}_{44} \end{array} \right], \end{aligned} \tag{3.3}$$

where the second-order partial derivatives of $\ell(\boldsymbol{\Theta}|\underline{\mathbf{y}})$, for $c = 1, 2$, are presented in Appendix B.

Under the asymptotic properties of MLE methodology, it is known that the $\hat{\boldsymbol{\Theta}}$ converges in distribution to a multivariate normal distribution centered at the true parameter vector $\boldsymbol{\Theta}$, with estimated variance-covariance matrix determined by the inverse observed Fisher information matrix, i.e., $\hat{\boldsymbol{\Theta}} \xrightarrow{d} N(\boldsymbol{\Theta}, \mathcal{I}^{-1}(\hat{\boldsymbol{\Theta}}))$, as $n \to \infty$. For practical inference, the $100(1-\alpha)\%$ ACIs for individual parameters λ_c and σ_c $(c = 1, 2)$ are constructed as:

$$\hat{\lambda}_c \pm z_{\alpha/2} \sqrt{\hat{V}_{cc}}, \text{ and } \hat{\sigma}_c \pm z_{\alpha/2} \sqrt{\hat{V}_{vv}}, v = c + 2, \ c = 1, 2,$$

where $z_{\alpha/2}$ is the upper $\alpha/2$ quantile of the standard normal distribution.

To construct the ACIs for the RF $S(t; \boldsymbol{\Theta})$ and FRF $h(t; \boldsymbol{\Theta})$, we first need to approximate the variances of the MLEs related to these functions using the delta method. This method employs a first-order Taylor expansion around the MLEs of the parameters λ_c and $\sigma_c, c = 1, 2$. The partial derivatives of $S(t; \boldsymbol{\Theta})$ and $h(t; \boldsymbol{\Theta})$ with respect to these parameters form gradient vectors that quantify their sensitivity to parameter variations. Below are the gradients derived from the RF and FRF, respectively, evaluated at MLEs by substituting $\lambda_c \to \hat{\lambda}_c$ and $\sigma_c \to \hat{\sigma}_c$,

$$\hat{\nabla}_S = -S(t; \hat{\boldsymbol{\Theta}}) \begin{bmatrix} \hat{\sigma}_1 t[\omega(t; \hat{\lambda}_c)]^{\hat{\sigma}_1 - 1} \\ [\omega(t; \hat{\lambda}_c)]^{\hat{\sigma}_1} \log[\omega(t; \hat{\lambda}_c)] \\ \hat{\sigma}_2 t[\omega(t; \hat{\lambda}_c)]^{\hat{\sigma}_2 - 1} \\ [\omega(t; \hat{\lambda}_c)]^{\hat{\sigma}_2} \log[\omega(t; \hat{\lambda}_c)] \end{bmatrix}$$

and

$$\hat{\nabla}_h = \begin{bmatrix} \hat{\sigma}_1 \left(1+\hat{\lambda}_1 t\right)^{\hat{\sigma}_1-2}\left(1+\hat{\lambda}_1\hat{\sigma}_1 t\right) \\ \hat{\lambda}_1 \left(1+\hat{\lambda}_1 t\right)^{\hat{\sigma}_1-1}\left[1+\hat{\sigma}_1 \ln\left(1+\hat{\lambda}_1 t\right)\right] \\ \hat{\sigma}_2 \left(1+\hat{\lambda}_2 t\right)^{\hat{\sigma}_2-2}\left(1+\hat{\lambda}_2\hat{\sigma}_2 t\right) \\ \hat{\lambda}_2 \left(1+\hat{\lambda}_2 t\right)^{\hat{\sigma}_2-1}\left[1+\hat{\sigma}_2 \ln\left(1+\hat{\lambda}_2 t\right)\right] \end{bmatrix}.$$

Then, the estimated variances of the MLEs of the RF and FRF can be computed as

$$\hat{V}_S \approx \hat{\nabla}_S^\top \mathcal{I}^{-1}(\hat{\boldsymbol{\Theta}})\hat{\nabla}_S \text{ and } \hat{V}_h \approx \hat{\nabla}_h^\top \mathcal{I}^{-1}(\hat{\boldsymbol{\Theta}})\hat{\nabla}_h.$$

As a result, the $100(1-\alpha)\%$ ACIs for the RF and FRF can be obtained as

$$\hat{S}(t) \pm z_{\alpha/2}\sqrt{\hat{V}_S} \text{ and } \hat{h}(t) \pm z_{\alpha/2}\sqrt{\hat{V}_h}.$$

4. Bayesian estimation

In recent years, Bayesian methodology has emerged as a widely adopted framework across disciplines such as engineering, biomedicine, and clinical research. Its ability to integrate existing knowledge with observed data proves particularly advantageous in reliability analysis, where limited datasets often constrain traditional approaches. This work develops Bayesian estimators and associated HPD credible interval ranges for the parameters λ_c, σ_c $(c = 1, 2)$, RF, and FRF of the NH competing risks model. While alternative loss functions remain applicable, we prioritize the squared error loss function for its analytical symmetry and widespread utility. Given the absence of conjugate priors for λ_c and $\sigma_c, c = 1, 2$, and the computational impracticality of Jeffreys priors due to intricate variance-covariance matrix, we utilize gamma distributions as priors for the various parameters. This choice is motivated by three factors: (1) The gamma distribution naturally accommodates the support of the parameters. (2) It simplifies calculations, simplifying implementation. (3) It reduces mathematical complexity, especially with models that contain a large number of parameters. Assume that $\lambda_c \sim Gamma(\tau_c, \kappa_c)$ and $\sigma_c \sim Gamma(a_c, b_c)$. The joint prior distribution of $\boldsymbol{\Theta}$ is then given by

$$\pi(\boldsymbol{\Theta}) \propto \prod_{c=1}^{2} \lambda_c^{\tau_c-1}\sigma_c^{a_c-1}e^{-\kappa_c\lambda_c-b_c\sigma_c}, \tag{4.1}$$

where $\tau_c, \kappa_c, a_c, b_c > 0$ are the hyperparameters, and assumed to be known.

4.1. Posterior distribution and Bayes estimators

Applying Bayes' theorem, the posterior distribution is obtained by combining the likelihood function specified in (3.1) with the joint prior distribution defined in (4.1). This joint posterior distribution satisfies the following proportionality relationship:

$$P(\boldsymbol{\Theta}|\underline{\mathbf{y}}) \propto L(\boldsymbol{\Theta}|\underline{\mathbf{y}})\,\pi(\boldsymbol{\Theta}),$$

which expands to

$$P(\boldsymbol{\Theta}|\underline{\mathbf{y}}) \propto \left[\prod_{c=1}^{2} \lambda_c^{D_c+\tau_c-1}\sigma_c^{D_c+a_c-1}\right]\exp\left\{\sum_{c=1}^{2}\sum_{i=1}^{D_c}(\sigma_c-1)\log[\omega(y_i;\lambda_c)] - \sum_{c=1}^{2}\sum_{i=1}^{D}[\omega(y_i;\lambda_c)]^{\sigma_c} - \sum_{c=1}^{2}\sum_{i=1}^{J} Q_i[\omega(y_i;\lambda_c)]^{\sigma_c} - \sum_{c=1}^{2} S^*[\omega(\eta;\lambda_c)]^{\sigma_c} - \sum_{c=1}^{2}(\kappa_c\lambda_c + b_c\sigma_c)\right\}, \tag{4.2}$$

For any function of $\boldsymbol{\Theta}$, say $g(\boldsymbol{\Theta})$, the Bayes estimator under the squared error loss is obtained using (4.2) as

$$\tilde{g}_{\text{Bayes}} = \int g(\boldsymbol{\Theta})P(\boldsymbol{\Theta}|\underline{\mathbf{y}})d\boldsymbol{\Theta}. \tag{4.3}$$

The Bayesian estimator defined in (4.3) involves solving analytically intractable integrals due to the high-dimensional and non-conjugate nature of the posterior distribution. To overcome this challenge, we employ Markov Chain Monte Carlo (MCMC) techniques to generate samples directly from the posterior distribution specified in (4.2). These samples facilitate the approximation of posterior expectations for Bayes estimates and enable the construction of the HPD credible interval ranges. A critical component of the MCMC implementation involves deriving the full conditional posterior distributions for each parameter. From the joint posterior in (4.2), the conditional distributions for λ_c and σ_c ($c = 1, 2$) are given by

$$P_1(\lambda_c|\boldsymbol{\Theta}_{-\lambda_c}, \underline{\mathbf{y}}) \propto \lambda_c^{D_c+\tau_c-1}\exp\left\{(\sigma_c-1)\sum_{i=1}^{D_c}(\sigma_c-1)\log[\omega(y_i;\lambda_c)] - \sum_{i=1}^{D}[\omega(y_i;\lambda_c)]^{\sigma_c} - \sum_{i=1}^{J} Q_i[\omega(y_i;\lambda_c)]^{\sigma_c} - S^*[\omega(\eta;\lambda_c)]^{\sigma_c} - \kappa_c\lambda_c\right\} \tag{4.4}$$

and

$$P_2(\sigma_c|\boldsymbol{\Theta}_{-\sigma_c}, \underline{\mathbf{y}}) \propto \sigma_c^{D_c+a_c-1}\exp\left\{\sigma_c\sum_{i=1}^{D_c}\log[\omega(y_i;\lambda_c)] - \sum_{i=1}^{D}[\omega(y_i;\lambda_c)]^{\sigma_c} - \sum_{i=1}^{J} Q_i[\omega(y_i;\lambda_c)]^{\sigma_c} - S^*[\omega(\eta;\lambda_c)]^{\sigma_c} - b_c\sigma_c\right\}. \tag{4.5}$$

An examination of the conditional distributions in (4.4) and (4.5) indicates that they diverge from standard parametric forms. This lack of conjugacy prevents the application of conventional sampling methods, such as inverse transform sampling, for direct sample generation. To address this computational challenge, we employ the MH algorithm, a fundamental MCMC technique, to iteratively approximate draws from these complex posterior conditionals.

4.2. Steps for implementing MH algorithm and Bayes estimates

The MH algorithm is a widely recognized MCMC procedure for sampling from complex or non-standard probability distributions. This algorithm employs a proposal distribution to generate candidate samples. In the context of this analysis, the normal distribution, characterized by its mean and variance,

is initialized using the MLEs of the parameters. The algorithm iteratively proposes new parameter values derived from this distribution and evaluates their acceptance probability, thereby ensuring that the generated Markov chain converges to the target posterior distribution. Key steps in the process include: (1) drawing a candidate sample from the normal proposal distribution; (2) computing the ratio of the candidate sample relative to the current state; and (3) accepting the candidate sample with a probability determined by the computed ratio; if the candidate is not accepted, the current state is retained. Subsequently, the MCMC iterative process constructs a dependent sequence of samples that asymptotically approximates the posterior distribution.

To justify and determine the validity of the posterior analysis, the use of normal proposal distributions for all parameters in the MH algorithm is examined by generating one independent IAPTIIC competing risks dataset (when $(n, m) = (100, 50)$, $(T_1, T_2) = (2, 5)$, and $Q_i = 1, i = 1, ..., m$) from NH(λ_i, σ_i), $i = 1, 2$ distribution at $(\lambda_1, \lambda_2, \sigma_1, \sigma_2) = (1.5, 0.5, 0.5, 1.5)$; see Figure 1. It shows that the fully conditional distributions of λ_i and σ_i (for $i = 1, 2$) provided in (4.4) and (4.5), respectively, using this collected sample behave similarly to the normal density.

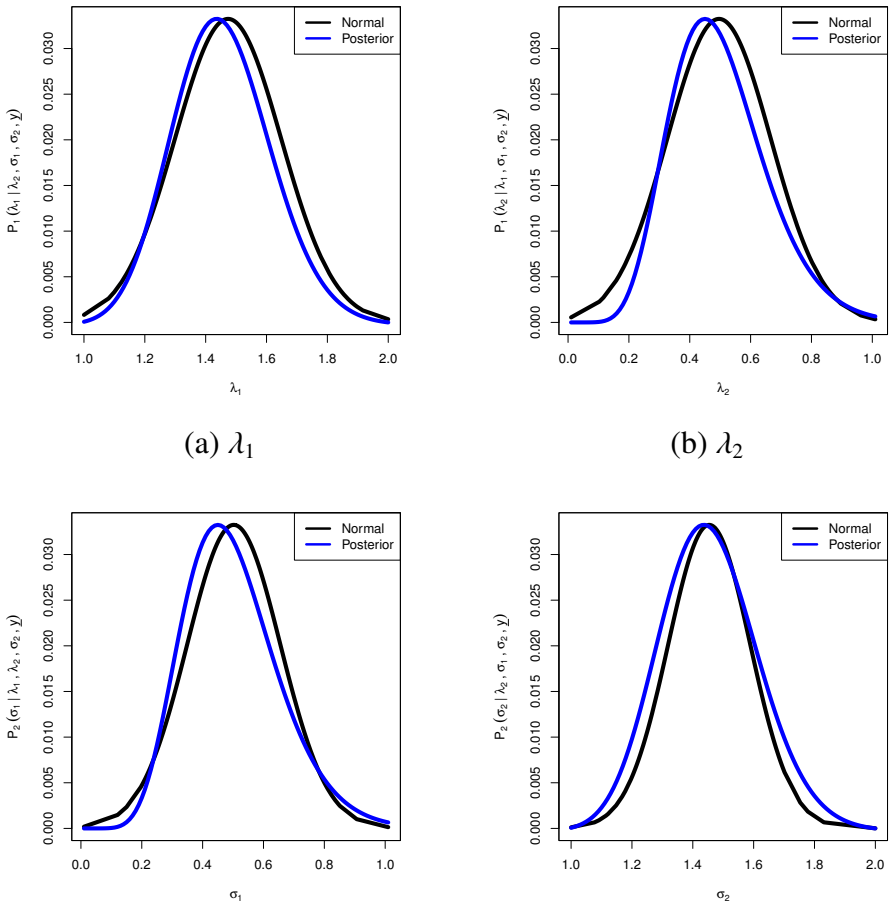

(a) λ_1 (b) λ_2

(c) σ_1 (d) σ_2

Figure 1. The normal and posterior density curves of λ_i and σ_i (for $i = 1, 2$).

The complete steps to generate the MCMC samples are given as

(1) Set initial values of $\lambda_c^{(0)}$ and $\sigma_c^{(0)}$ using the associated MLEs.
(2) Perform the following MH steps: For each iteration $k = 1, \ldots, \mathcal{K}$:

- For $c = 1, 2$:
  (a) Simulate $\lambda_c^* \sim \mathrm{N}(\hat{\lambda}_c, \hat{V}_{cc})$.
  (b) Compute the acceptance probability:

$$\xi_{\lambda_c} = \min\left(1, \frac{P_1(\lambda_c^*|\boldsymbol{\Theta}_{-\lambda_c}^{(k-1)}, \underline{\mathbf{y}})}{P_1(\lambda_c^{(k-1)}|\boldsymbol{\Theta}_{-\lambda_c}^{(k-1)}, \underline{\mathbf{y}})}\right).$$

  (c) Accept/reject: $\lambda_c^{(k)} = \begin{cases} \lambda_c^* & \text{with probability } \xi_{\lambda_c} \\ \lambda_c^{(k-1)} & \text{otherwise} \end{cases}$.
  (d) Simulate $\sigma_c^* \sim \mathrm{N}(\hat{\sigma}_c, \hat{V}_{vv})$.
  (e) Compute the acceptance probability:

$$\xi_{\sigma_c} = \min\left(1, \frac{P_2(\sigma_c^*|\boldsymbol{\Theta}_{-\sigma_c}^{(k)}, \underline{\mathbf{y}})}{P_2(\sigma_c^{(k-1)}|\boldsymbol{\Theta}_{-\sigma_c}^{(k)}, \underline{\mathbf{y}})}\right).$$

  (f) Accept/reject: $\sigma_c^{(k)} = \begin{cases} \sigma_c^* & \text{with probability } \xi_{\sigma_c} \\ \sigma_c^{(k-1)} & \text{otherwise} \end{cases}$.

(3) Obtain the RF and FRF as:

$$S^{(k)} = \exp\left\{2 - \sum_{c=1}^{2}[\omega(t; \lambda_c^{(k)})]^{\sigma_c^{(k)}}\right\} \text{ and } h^{(k)} = \sum_{c=1}^{2}\lambda_c^{(k)}\sigma_c^{(k)}[\omega(y; \lambda_c^{(k)})]^{\sigma_c^{(k)}-1}.$$

(4) Discard the first B samples as burn-in to assure the convergence of the chain. Then, store the remaining sequence as

$$\left\{\lambda_1^{(k)}, \lambda_2^{(k)}, \sigma_1^{(k)}, \sigma_2^{(k)}, S^{(k)}, h^{(k)}\right\}, \quad k = B+1, \ldots, \mathcal{K}.$$

The Bayesian inference results for the parameter λ_1, as an example, including both the point estimate and the HPD credible interval are derived from the acquired MCMC samples. Under the squared error loss function, the Bayes estimate of λ_1 is calculated as the posterior mean, obtained by

$$\hat{\lambda}_1 = \frac{1}{\mathcal{K} - B}\sum_{k=B+1}^{\mathcal{K}}\lambda_1^{(k)}.$$

The $100(1-\alpha)\%$ HPD credible interval is computed as follows:

(1) Arrange $\{\lambda_1^{(B+1)}, \ldots, \lambda_1^{(\mathcal{K})}\}$ in ascending order to get $\lambda_1^{[B+1]} \leq \lambda_1^{[2]} \leq \cdots \leq \lambda_1^{[\mathcal{K}]}$.
(2) Calculate the number of samples to exclude $r = [\alpha(\mathcal{K} - B)]$, .
(3) Obtain the HPD interval as $\left\{\lambda_1^{[i]}, \lambda_1^{[i+(\mathcal{K}-B-r)]}\right\}$ with the smallest range:

$$\arg\min_{1 \leq i \leq r}\left(\lambda_1^{[i+(\mathcal{K}-B-r)]} - \lambda_1^{[i]}\right).$$

5. Monte Carlo comparisons

This section conducts a comprehensive Monte Carlo simulation study to rigorously evaluate the efficacy of the theoretical inferences of λ_i, σ_i (for $i = 1, 2$), $S(t)$, and $h(t)$ derived in preceding sections. The focus is on assessing the accuracy and precision of both point and interval estimators for the NH(λ_i, σ_i), $i = 1, 2$ competing risk model parameters, alongside the RF $S(t)$ and FRF $h(t)$. To achieve that, we simulate 1,000 independent IAPTIIC competing risks datasets from the NH(λ_i, σ_i), $i = 1, 2$ distribution, when $(\lambda_1, \lambda_2, \sigma_1, \sigma_2) = (1.5, 0.5, 0.5, 1.5)$. At a predetermined time point, $t = 0.1$, the estimated values of $(S(t), h(t))$ are computed and compared against their respective true values of 0.86216 and 0.53749. The simulation framework is done utilizing various experimental configurations, incorporating different values of the threshold levels T_i, $i = 1, 2$, the total number of units under study n, the effective sample size m, and the removal strategy $\mathbf{Q}$. To analyze the impact of different censoring schemes $\mathbf{Q}$ on the estimator performance, besides several combinations of $T_1 \in \{0.5, 1.0\}$ and $T_2 \in \{1.0, 1.5\}$, different removal patterns $\mathbf{Q}$ are taken into account; see Table 1. To distinguish, $\mathbf{Q} = (2^{10}, 0^{10})$ (for instance) means that two survivors are randomly removed during the first ten stages of censoring, and removal stops in the remaining stages.

Table 1. Different patterns of $\mathbf{Q}$ in Monte Carlo simulations.

Design no.	Style	
$(n, m) \rightarrow$	(40,20)	(40,30)
1	$(2^{10}, 0^{10})$	$(2^5, 0^{25})$
2	$(0^5, 2^{10}, 0^5)$	$(0^{12}, 2^5, 0^{13})$
3	$(0^{10}, 2^{10})$	$(0^{25}, 2^5)$
$(n, m) \rightarrow$	(80,40)	(80,60)
1	$(2^{20}, 0^{20})$	$(2^{10}, 0^{50})$
2	$(0^{10}, 2^{20}, 0^{10})$	$(0^{25}, 2^{10}, 0^{25})$
3	$(0^{20}, 2^{20})$	$(0^{50}, 2^{10})$

To get IAPTIIC competing risk data from the NH(λ_i, σ_i), $i = 1, 2$ competing risk populations, beyond assign the corresponding values for T_i, $i = 1, 2$, n, m, and $\mathbf{Q}$, do the following steps:

Step 1. Define the true values of NH model parameters λ_i and σ_i for $i = 1, 2$.

Step 2. Simulate a conventional PTIIC competing risk dataset as follows:

(a) Draw m independent random samples, say $g_1, g_2, \ldots, g_m$, from a uniform $U(0, 1)$ model.
(b) Set $v_i = g_i^{\left(i+\sum_{j=m-i+1}^{m} Q_j\right)^{-1}}$, $\quad i = 1, 2, \ldots, m$.
(c) Set $U_i = 1 - v_m v_{m-1} \cdots v_{m-i+1}$, $\quad i = 1, 2, \ldots, m$.
(d) Set $Y_i = F^{-1}(U_i; \lambda_i, \sigma_i)$, $\quad j = 1, 2$, $i = 1, 2, \ldots, m$.

Step 3. Identify the truncation point d_1 at T_1, and for cases II and III, discard all failure times beyond this threshold, i.e., Y_i, $i = d_1 + 2, \ldots, m$.

Step 4. Generate the first $m - d_1 - 1$ order statistics from a truncated PDF, given by $f(y)\left[S\left(y_{d_1+1}\right)\right]^{-1}$, where the sample size is determined as $n - d_1 - 1 - \sum_{i=1}^{d_1} Q_i$, resulting in ordered observations $Y_{d_1+2}, \ldots, Y_m$.

Step 5. Assign a cause-of-failure indicator for each observation, using the indicator $\delta_i,\ i = 1, 2$ to classify risks as cause 1 or 2.

For each simulated dataset, the MLEs and the associated ACIs at a nominal 95% confidence level are computed for the NH distribution parameters λ_i and σ_i (for $i = 1, 2$), as well as the reliability features $S(t)$ and $h(t)$. Following Henningsen and Toomet [29], the NR method is employed for MLE computation, using the `maxLik` package in R version 4.2.2. Moreover, Bayesian analysis—both point estimates and 95% HPD intervals—are obtained via MCMC simulations using the coda package suggested by Plummer et al. [30].

For the Bayesian analysis, two informative prior groups for (τ_i, κ_i) (of λ_i) and for (a_i, b_i) (of σ_i) for $i = 1, 2$, are considered as follows:

- **Group A**: $(\tau_1, \tau_2, a_1, b_2) = (7.5, 2.5, 2.5, 7.5)$ and $\kappa_i = b_i = 5,\ i = 1, 2$;
- **Group B**: $(\tau_1, \tau_2, a_1, b_2) = (15, 5, 5, 15)$ and $\kappa_i = b_i = 10,\ i = 1, 2$.

It is better to mention here that the values assigned in prior groups A and B ensure that their means align with the true values of the NH competing risk parameters λ_i and σ_i for $i = 1, 2$. In practical applications, if prior knowledge regarding parameter values is unavailable, frequentist estimates are often preferred due to the computational burden of Bayesian methods. Following the MCMC approach outlined in Section 4, a total of $\mathcal{K} = 12,000$ MCMC samples are generated, with the first iterations $B = 2,000$ discarded as the burn-in phase. Subsequently, the remaining 10,000 samples are then used to derive Bayesian point estimates and the corresponding 95% HPD intervals.

For performance evaluation, the average estimates (AEs) of $\lambda_i, i = 1, 2$, $\sigma_i, i = 1, 2$, $S(t)$, or $h(t)$ (say, ϱ) are computed as follows:

$$\mathrm{AE}_{\breve{\varrho}} = \frac{1}{1000}\sum_{i=1}^{1000} \breve{\varrho}^{[i]},$$

where $\breve{\varrho}^{[i]}$ represents the estimate of ϱ from the ith simulated dataset.

The precision of the point estimates is assessed using the root mean squared error (RMSE) and the average relative absolute bias (ARAB), defined as:

$$\mathrm{RMSE}\left(\breve{\varrho}\right) = \sqrt{\frac{1}{1000}\sum\nolimits_{i=1}^{1000}\left(\breve{\varrho}^{[i]} - \varrho\right)^2},$$

$$\mathrm{ARAB}\left(\breve{\varrho}\right) = \frac{1}{1000}\sum\nolimits_{i=1}^{1000} \varrho^{-1}\left|\breve{\varrho}^{[i]} - \varrho\right|,$$

respectively.

Interval estimates are evaluated based on their average interval lengths (AILs) and coverage probabilities (CPs), defined as:

$$\mathrm{AIL}^{95\%}\left(\varrho\right) = \frac{1}{1000}\sum\nolimits_{i=1}^{1000}\left(U_{\hat{\varrho}^{[i]}} - L_{\hat{\varrho}^{[i]}}\right),$$

$$\mathrm{CP}^{95\%}(\varrho) = \frac{1}{1000}\sum_{i=1}^{1000} \mathsf{q}_{\left(L_{\hat{\varrho}[i]};U_{\hat{\varrho}[i]}\right)}(\varrho),$$

where $\mathsf{q}(\cdot)$ denotes the indicator function, and $L(\cdot)$ and $U(\cdot)$ correspond to the lower and upper bounds of the 95% ACI (or HPD) interval for ϱ.

Tables 2–7 present the AEs, RMSEs, and ARABs of $\lambda_i,\ i = 1, 2, \sigma_i,\ i = 1, 2, S(t)$, or $h(t)$ in the first, second, and third columns, respectively. Likewise, the AILs and CPs of the same unknown subjects are reported in the first and second columns, respectively; see Tables 8–13.

Several observations on the behavior of $\lambda_i,\ i = 1, 2, \sigma_i,\ i = 1, 2, S(t)$, and $h(t)$, from Tables 2–13, in terms of minimum RMSE, ARAB, and AIL values as well as maximum CP values, are presented as follows:

- The proposed point estimates and 95% interval estimators for $\lambda_i,\ i = 1, 2, \sigma_i,\ i = 1, 2, S(t)$, or $h(t)$ demonstrate good and reliable performance.
- As n increases, the accuracy of all estimates derived from the likelihood or Bayes approach improves. A similar trend is observed when the total number of failures $\sum_{i=1}^{m} Q_i$ (or, equivalently, $n - m$) is reduced.
- When $T_i,\ i = 1, 2$, increases, it is noted that:
  - The RMSEs and ARABs for all estimates of λ_i and σ_i (for $i = 1, 2$) as well as of $S(t)$ and $h(t)$ decrease;
  - The AILs for 95% ACI (or HPD) estimates of $\lambda_i,\ i = 1, 2, \sigma_i,\ i = 1, 2, S(t)$, or $h(t)$ decrease;
  - The CPs corresponding to $\lambda_i,\ i = 1, 2, \sigma_i,\ i = 1, 2, S(t)$, and $h(t)$ generally increase.
- Evaluating the performance of different censoring scenarios $Q_i,\ i = 1, 2, \ldots, m$, it reveals that:
  - All estimates of $\sigma_i,\ i = 1, 2$ achieve optimal performance when censoring occurs in the earlier stages, i.e., design #1;
  - All estimates of $\lambda_i,\ i = 1, 2$, and $h(t)$ achieve optimal performance when censoring occurs in the late stages, i.e., design #3;
  - All estimates of $S(t)$ achieve optimal performance when censoring occurs in the middle stages, i.e., design #2.
- Bayesian estimators (or HPD intervals) for $\lambda_i,\ i = 1, 2, \sigma_i,\ i = 1, 2, S(t)$, or $h(t)$ outperform their maximum likelihood (or ACI) counterparts due to the use of informative gamma priors.
- Since prior group B has lower variance than its competitors A, Bayesian estimates derived using group B exhibit efficient results.
- Finally, for an improved Type-II adaptive progressive censored competing risks framework, the Bayesian MH approach is recommended for estimating both the model competing risk parameters λ_i and σ_i (for $i = 1, 2$) and reliability characteristics $S(t)$ and $h(t)$ of the NH lifespan model.

As a summary, the simulation finds that the proposed point and interval estimators for λ_i, σ_i, $S(t)$, and $h(t)$ perform reliably, with improved accuracy as sample size (n) increases or the number of failures (m) decreases. Performance also improves with higher $T_i,\ i = 1, 2$ values, as RMSE, ARAB, and AIL values decrease while CP increases, and optimal censoring designs vary for different parameters. Bayesian methods, especially those using informative priors from group B, consistently outperform likelihood-based approaches, with the Bayesian MH method recommended for enhanced estimation in the adaptive progressive censoring framework.

Table 2. The maximum likelihood and Bayesian estimation results of λ_1.

(n, m)	Design	MLE			Bayes					
		AE	RMSE	ARAB	AE	RMSE	ARAB	AE	RMSE	ARAB
Group→					A			B		
					$(T_1, T_2) = (0.5, 1.0)$					
(40,20)	1	1.8578	1.3535	0.8758	1.3851	0.7183	0.4430	0.8494	0.4148	0.2609
	2	2.0144	1.2343	0.8691	1.3695	0.7057	0.4338	0.8355	0.3514	0.2141
	3	1.6456	1.1848	0.8058	1.8656	0.3282	0.1642	1.5251	0.2941	0.1601
(40,30)	1	1.5485	0.6423	0.7513	1.5330	0.2359	0.1433	1.3851	0.2310	0.1287
	2	1.4723	0.6955	0.7819	1.5740	0.3147	0.1552	1.4238	0.2498	0.1411
	3	1.8994	0.5791	0.5722	1.5241	0.2340	0.1317	1.6589	0.2250	0.1130
(80,40)	1	1.2113	0.5243	0.5303	1.6079	0.2330	0.1231	1.6763	0.2203	0.1063
	2	1.3230	0.5031	0.5071	1.5834	0.2210	0.1106	1.6701	0.2122	0.0996
	3	1.6923	0.4710	0.4838	1.3433	0.2077	0.1026	1.5353	0.1946	0.0950
(80,60)	1	1.4136	0.4445	0.3595	1.6326	0.1878	0.0932	1.6144	0.1550	0.0770
	2	1.2274	0.4488	0.4207	1.6505	0.1988	0.1016	1.6162	0.1783	0.0892
	3	1.9921	0.3538	0.3135	1.8184	0.1507	0.0817	1.3114	0.1380	0.0726
					$(T_1, T_2) = (1.0, 1.5)$					
(40,20)	1	1.5071	1.2634	0.8346	1.4085	0.6957	0.3770	0.8880	0.4829	0.2959
	2	1.7100	1.1427	0.8037	1.4136	0.6673	0.3141	0.8586	0.4377	0.2668
	3	1.8677	0.8440	0.6696	1.8293	0.4494	0.2813	1.4645	0.3914	0.2470
(40,30)	1	1.2617	0.4847	0.4958	1.5836	0.2610	0.1481	1.4236	0.2389	0.1434
	2	1.3270	0.6317	0.5078	1.5817	0.4414	0.2631	1.4137	0.3326	0.2016
	3	1.5992	0.4628	0.4261	1.5384	0.2359	0.1361	1.6528	0.2328	0.1306
(80,40)	1	1.4830	0.4108	0.4020	1.2996	0.2264	0.1208	1.8763	0.1958	0.1016
	2	1.7962	0.3926	0.3678	1.3101	0.2143	0.1108	1.8814	0.1759	0.0907
	3	1.3698	0.2842	0.3275	1.6140	0.2013	0.1063	1.2934	0.1685	0.0835
(80,60)	1	1.3879	0.2427	0.3004	1.8670	0.1707	0.0894	1.3730	0.1541	0.0800
	2	1.8717	0.2556	0.3153	1.9193	0.1877	0.0933	1.4186	0.1579	0.0801
	3	1.6396	0.2200	0.2817	1.7819	0.1529	0.0803	1.6031	0.1505	0.0764

Table 3. The maximum likelihood and Bayesian estimation results of λ_2.

(n, m)	Design	MLE			Bayes					
		AE	RMSE	ARAB	AE	RMSE	ARAB	AE	RMSE	ARAB
Group→					A			B		
					$(T_1, T_2) = (0.5, 1.0)$					
(40,20)	1	0.6893	1.2878	1.3380	0.5654	0.5343	0.8462	0.4754	0.3819	0.6347
	2	0.7125	1.0307	1.1972	0.6016	0.5174	0.7798	0.5138	0.3642	0.5190
	3	0.5062	0.9570	0.9698	0.6520	0.3485	0.5222	0.7473	0.3141	0.4726
(40,30)	1	0.6309	0.7844	0.8948	0.6606	0.2995	0.3985	0.7054	0.2942	0.3686
	2	0.6794	0.8489	0.9244	0.7557	0.3075	0.4431	0.7996	0.3058	0.3903
	3	0.8536	0.6327	0.8243	0.5271	0.2903	0.3264	0.5652	0.2656	0.3014
(80,40)	1	0.4999	0.6040	0.7541	0.6321	0.2574	0.2894	0.6197	0.2373	0.2882
	2	0.5287	0.5523	0.7487	0.6030	0.2523	0.2778	0.5934	0.2211	0.2694
	3	0.4713	0.4616	0.6748	0.4385	0.2466	0.2525	0.4476	0.1786	0.2402
(80,60)	1	0.5314	0.4171	0.6686	0.9206	0.1737	0.2227	0.7214	0.1572	0.2042
	2	0.5861	0.4449	0.6722	0.8870	0.2429	0.2296	0.6988	0.1616	0.2252
	3	0.9666	0.4093	0.6273	0.5481	0.1665	0.1925	0.4901	0.1512	0.1884
					$(T_1, T_2) = (1.0, 1.5)$					
(40,20)	1	0.5558	1.1159	0.7663	0.7112	0.4220	0.6497	0.5686	0.3732	0.6160
	2	0.4947	0.9036	0.7466	0.6154	0.3631	0.5957	0.5158	0.3549	0.5311
	3	0.3996	0.7290	0.6746	0.5386	0.3540	0.5175	0.6508	0.3113	0.3934
(40,30)	1	0.4975	0.5233	0.6417	0.7609	0.3420	0.4121	0.7913	0.2669	0.3238
	2	0.5865	0.5722	0.6613	0.7532	0.3493	0.4245	0.7802	0.2817	0.3852
	3	0.7114	0.4109	0.5762	0.5940	0.3121	0.3536	0.6313	0.2515	0.3179
(80,40)	1	0.3922	0.4098	0.5362	0.6254	0.2809	0.3416	0.4730	0.2190	0.3107
	2	0.3434	0.3503	0.4750	0.6112	0.2557	0.3142	0.4593	0.2105	0.2557
	3	0.6227	0.3378	0.4286	0.8110	0.2543	0.3062	0.5069	0.2020	0.2358
(80,60)	1	0.4386	0.3205	0.3118	0.6512	0.2214	0.2493	0.6474	0.1623	0.2116
	2	0.5239	0.3234	0.4184	0.6937	0.2218	0.2902	0.6902	0.1975	0.2216
	3	0.7229	0.2266	0.2934	0.6228	0.1922	0.2304	0.5045	0.1565	0.2075

Table 4. The maximum likelihood and Bayesian estimation results of σ_1.

(n, m)	Design	MLE			Bayes					
		AE	RMSE	ARAB	AE	RMSE	ARAB	AE	RMSE	ARAB
Group→					A			B		
$(T_1, T_2) = (0.5, 1.0)$										
(40,20)	1	0.5041	0.9142	1.1432	0.6142	0.2159	0.4071	0.6879	0.2024	0.3720
	2	0.6484	0.9646	1.3523	0.6293	0.2467	0.4468	0.6764	0.2288	0.4084
	3	0.7189	0.9500	1.2738	0.7740	0.2320	0.4191	0.6347	0.2106	0.3861
(40,30)	1	0.4270	0.8206	0.7696	0.6431	0.1980	0.3648	0.4200	0.1627	0.3089
	2	0.7220	0.8527	0.8211	0.8021	0.2038	0.3727	0.4456	0.1792	0.3261
	3	0.5804	0.8945	0.9865	0.5272	0.2134	0.3872	0.5241	0.1942	0.3471
(80,40)	1	0.4972	0.6573	0.5041	0.5300	0.1386	0.2421	0.3192	0.1210	0.2011
	2	0.4858	0.7770	0.6260	0.4012	0.1706	0.2691	0.4146	0.1320	0.2239
	3	0.6890	0.7944	0.6738	0.5402	0.1975	0.3125	0.4551	0.1466	0.2866
(80,60)	1	0.6131	0.4215	0.2456	0.4314	0.1149	0.1780	0.3704	0.0792	0.1473
	2	0.6286	0.5886	0.4851	0.6324	0.1278	0.2204	0.3345	0.1123	0.1711
	3	0.5827	0.4801	0.3242	0.4339	0.1190	0.1852	0.3435	0.0983	0.1665
$(T_1, T_2) = (1.0, 1.5)$										
(40,20)	1	0.4040	0.5898	1.1078	0.4871	0.1825	0.4193	0.5560	0.1792	0.3158
	2	0.6741	0.6122	1.1730	0.3356	0.2547	0.4525	0.7070	0.1959	0.3472
	3	0.7167	0.6798	1.2564	0.3608	0.2877	0.4953	0.7473	0.2194	0.3846
(40,30)	1	0.6989	0.3469	0.7423	0.5389	0.1460	0.2001	0.5170	0.1119	0.1811
	2	0.3814	0.5697	0.8135	0.4914	0.1652	0.3236	0.5594	0.1362	0.2340
	3	0.4898	0.3775	0.9267	0.5055	0.1525	0.2344	0.5720	0.1218	0.1907
(80,40)	1	0.6810	0.1963	0.4894	0.3660	0.1073	0.1726	0.4180	0.1000	0.1534
	2	0.7160	0.2499	0.5932	0.5291	0.1184	0.1763	0.4523	0.1013	0.1685
	3	0.5125	0.3194	0.6055	0.5347	0.1217	0.1826	0.4626	0.1039	0.1763
(80,60)	1	0.5621	0.1067	0.2195	0.4563	0.0837	0.1365	0.4422	0.0816	0.1233
	2	0.7024	0.1621	0.4554	0.6036	0.1037	0.1668	0.6614	0.0987	0.1462
	3	0.4767	0.1338	0.3080	0.5525	0.0949	0.1594	0.6151	0.0847	0.1343

Table 5. The maximum likelihood and Bayesian estimation results of σ_2.

(n, m)	Design	MLE			Bayes					
		AE	RMSE	ARAB	AE	RMSE	ARAB	AE	RMSE	ARAB
Group→					A			B		
$(T_1, T_2) = (0.5, 1.0)$										
(40,20)	1	1.3267	0.9831	1.3767	1.3615	0.5438	0.3387	0.9856	0.3835	0.1939
	2	1.8744	1.2025	1.4704	1.2084	0.5516	0.3430	1.3997	0.4778	0.2746
	3	1.7625	1.0695	1.4150	1.2291	0.5549	0.3602	1.4543	0.4830	0.2769
(40,30)	1	1.8045	0.7225	1.2195	1.3619	0.3408	0.1766	1.3117	0.3112	0.1364
	2	1.6446	0.7918	1.2829	1.1947	0.3659	0.1845	1.1494	0.3138	0.1413
	3	1.4407	0.8738	1.3479	1.2714	0.3799	0.1999	1.2199	0.3258	0.1548
(80,40)	1	1.6272	0.3821	0.8999	1.3985	0.3132	0.1458	1.4223	0.2890	0.1071
	2	1.8717	0.4367	1.0043	1.2398	0.3236	0.1547	1.3028	0.2928	0.1138
	3	1.4034	0.5883	1.1883	1.2537	0.3301	0.1659	1.3155	0.3010	0.1279
(80,60)	1	1.6291	0.2850	0.6460	1.4794	0.2542	0.0988	1.5636	0.2427	0.0846
	2	1.7382	0.3429	0.8385	1.3001	0.3050	0.1280	1.3502	0.2751	0.1011
	3	1.5277	0.3152	0.7691	1.2974	0.2887	0.1142	1.3615	0.2653	0.0867
$(T_1, T_2) = (1.0, 1.5)$										
(40,20)	1	1.6722	0.9204	1.0088	1.2491	0.4063	0.2100	1.0517	0.3615	0.1884
	2	1.9203	1.0142	1.1309	1.2366	0.4883	0.2989	1.3822	0.4160	0.2123
	3	1.6357	1.1435	1.2110	1.2597	0.4184	0.2354	1.3789	0.4105	0.2078
(40,30)	1	1.2765	0.6775	0.7032	1.4775	0.3466	0.1753	1.4045	0.3426	0.1572
	2	1.2864	0.7923	0.9422	1.2634	0.3640	0.1837	1.2272	0.3783	0.1834
	3	1.7853	0.7228	0.8796	1.2773	0.3558	0.1781	1.2360	0.3648	0.1737
(80,40)	1	1.7651	0.3826	0.2807	1.0868	0.3259	0.1463	1.4638	0.2302	0.1010
	2	1.3203	0.4133	0.3513	1.2710	0.3397	0.1548	1.9200	0.2842	0.1121
	3	1.3232	0.6105	0.4266	1.2781	0.3412	0.1686	1.9094	0.2957	0.1240
(80,60)	1	1.5971	0.1584	0.1283	1.0885	0.1318	0.0906	1.2438	0.1175	0.0671
	2	1.8682	0.2754	0.2158	1.5744	0.2731	0.1185	1.4607	0.2110	0.0803
	3	1.4591	0.1966	0.1931	1.4953	0.1882	0.0949	1.3911	0.1766	0.0771

Table 6. The maximum likelihood and Bayesian estimation results of $S(t)$.

(n,m)	Design	MLE			Bayes					
		AE	RMSE	ARAB	AE	RMSE	ARAB	AE	RMSE	ARAB
Group→					A			B		
					$(T_1, T_2) = (0.5, 1.0)$					
(40,20)	1	0.8088	0.1259	0.1081	0.9009	0.0505	0.0559	0.8886	0.0401	0.0440
	2	0.8045	0.0866	0.0715	0.8231	0.0441	0.0452	0.8358	0.0326	0.0326
	3	0.8225	0.1013	0.0916	0.8981	0.0482	0.0493	0.8875	0.0374	0.0382
(40,30)	1	0.7922	0.0760	0.0668	0.8536	0.0420	0.0420	0.8466	0.0309	0.0310
	2	0.7542	0.0738	0.0583	0.8789	0.0290	0.0291	0.8728	0.0239	0.0226
	3	0.8075	0.0724	0.0598	0.8801	0.0409	0.0335	0.8723	0.0290	0.0242
(80,40)	1	0.8165	0.0671	0.0569	0.8672	0.0270	0.0266	0.8590	0.0218	0.0206
	2	0.8140	0.0559	0.0495	0.9103	0.0205	0.0212	0.9001	0.0189	0.0163
	3	0.8286	0.0592	0.0523	0.8776	0.0216	0.0221	0.8689	0.0201	0.0194
(80,60)	1	0.7956	0.0584	0.0479	0.8542	0.0190	0.0194	0.8684	0.0173	0.0153
	2	0.7706	0.0454	0.0366	0.8820	0.0145	0.0137	0.8872	0.0122	0.0109
	3	0.8123	0.0520	0.0420	0.8485	0.0157	0.0150	0.8637	0.0146	0.0133
					$(T_1, T_2) = (1.0, 1.5)$					
(40,20)	1	0.8117	0.0904	0.0755	0.8729	0.0523	0.0648	0.8652	0.0396	0.0423
	2	0.8477	0.0747	0.0592	0.8641	0.0398	0.0572	0.8694	0.0287	0.0301
	3	0.8274	0.0798	0.0722	0.8881	0.0452	0.0602	0.8798	0.0324	0.0364
(40,30)	1	0.7878	0.0696	0.0548	0.8488	0.0328	0.0521	0.8443	0.0233	0.0282
	2	0.8265	0.0556	0.0455	0.8496	0.0260	0.0317	0.8460	0.0190	0.0206
	3	0.8087	0.0602	0.0525	0.8449	0.0277	0.0415	0.8404	0.0209	0.0246
(80,40)	1	0.8179	0.0550	0.0434	0.8658	0.0251	0.0267	0.8462	0.0179	0.0178
	2	0.8535	0.0415	0.0340	0.8732	0.0227	0.0230	0.8853	0.0170	0.0157
	3	0.8342	0.0514	0.0412	0.8682	0.0240	0.0252	0.8497	0.0176	0.0167
(80,60)	1	0.7901	0.0399	0.0314	0.8063	0.0215	0.0208	0.8258	0.0165	0.0155
	2	0.8358	0.0280	0.0214	0.8711	0.0179	0.0177	0.8823	0.0159	0.0140
	3	0.8100	0.0357	0.0276	0.8265	0.0202	0.0192	0.8430	0.0161	0.0151

Table 7. The maximum likelihood and Bayesian estimation results of $h(t)$.

(n,m)	Design	MLE			Bayes					
		AE	RMSE	ARAB	AE	RMSE	ARAB	AE	RMSE	ARAB
Group→					A			B		
					$(T_1, T_2) = (0.5, 1.0)$					
(40,20)	1	0.7531	0.8980	0.8071	0.8934	0.3977	0.4444	0.7408	0.3159	0.4198
	2	0.9252	0.9029	0.8834	0.2476	0.6513	0.6948	0.9099	0.3578	0.2350
	3	1.0868	0.8560	0.6035	0.2477	0.2712	0.4128	0.6993	0.2500	0.3818
(40,30)	1	1.0946	0.8283	0.5871	0.5844	0.3105	0.5403	0.6683	0.2318	0.3815
	2	0.9233	0.7140	0.5483	0.3786	0.2300	0.3793	0.4441	0.1990	0.3314
	3	1.8780	0.6879	0.4725	0.4006	0.2204	0.3583	0.4346	0.1849	0.3125
(80,40)	1	0.7200	0.6186	0.4300	0.4024	0.1707	0.2679	0.4702	0.1572	0.2543
	2	0.8606	0.6352	0.4498	0.4824	0.1718	0.2769	0.5528	0.1690	0.2710
	3	0.9517	0.4992	0.3734	0.2081	0.1621	0.2549	0.2574	0.1559	0.2400
(80,60)	1	1.0777	0.4844	0.3630	0.5073	0.1619	0.2532	0.4347	0.1477	0.2265
	2	0.8955	0.4814	0.3271	0.5507	0.1601	0.2486	0.4660	0.1254	0.1742
	3	1.3425	0.3417	0.2462	0.3665	0.1530	0.2449	0.3271	0.1026	0.1477
					$(T_1, T_2) = (1.0, 1.5)$					
(40,20)	1	0.9444	0.7456	0.6444	1.1369	0.3384	0.4259	0.3440	0.2893	0.4121
	2	1.1667	0.8718	1.1162	0.4108	0.4090	0.6622	0.3469	0.3973	0.5259
	3	1.1746	0.6306	0.4312	0.6388	0.3117	0.5405	0.7847	0.2624	0.3917
(40,30)	1	0.5718	0.6106	0.3606	0.4166	0.2355	0.3185	0.3535	0.2040	0.2438
	2	0.9515	0.5256	0.3498	0.5051	0.2311	0.2743	0.7204	0.1833	0.1961
	3	0.8780	0.5176	0.3459	0.6771	0.2282	0.3440	0.6856	0.1638	0.2579
(80,40)	1	0.7525	0.4499	0.3125	0.8828	0.2025	0.2179	0.3722	0.1530	0.1498
	2	0.8309	0.4685	0.3602	0.4523	0.2158	0.3436	0.6686	0.1600	0.2475
	3	0.7212	0.3391	0.3055	0.4869	0.1890	0.3045	0.6517	0.1410	0.2174
(80,60)	1	0.7534	0.3200	0.6322	0.6448	0.1818	0.2975	0.4046	0.1404	0.2132
	2	0.5693	0.2652	0.4404	0.4949	0.1809	0.2824	0.4678	0.1378	0.2109
	3	0.9056	0.2028	0.6546	0.3228	0.1540	0.2465	0.5145	0.1341	0.2087

Table 8. The 95% ACI/HPD estimation results of λ_1.

(n,m)	Design	ACI		HPD				ACI		HPD			
				Group A		Group 2				Group A		Group B	
		AIL	CP	AIL	CP	AIL	CP	AIL	CP	AIL	CP	AIL	CP
		$(T_1,T_2)=(0.5,1.0)$						$(T_1,T_2)=(1.0,1.5)$					
(40,20)	1	1.960	0.902	0.962	0.925	0.913	0.927	1.854	0.907	0.893	0.928	0.819	0.929
	2	1.794	0.907	0.913	0.927	0.872	0.929	1.651	0.912	0.828	0.930	0.758	0.931
	3	1.657	0.909	0.900	0.927	0.727	0.931	1.368	0.914	0.713	0.931	0.709	0.934
(40,30)	1	1.255	0.916	0.695	0.935	0.616	0.937	0.983	0.921	0.637	0.936	0.603	0.938
	2	1.414	0.912	0.766	0.932	0.664	0.935	1.176	0.917	0.694	0.934	0.637	0.936
	3	1.177	0.920	0.653	0.937	0.587	0.939	0.851	0.926	0.605	0.939	0.579	0.941
(80,40)	1	1.092	0.922	0.640	0.939	0.562	0.941	0.787	0.928	0.577	0.941	0.547	0.943
	2	0.854	0.926	0.581	0.941	0.548	0.943	0.707	0.932	0.565	0.942	0.506	0.944
	3	0.765	0.929	0.528	0.942	0.521	0.945	0.651	0.935	0.515	0.944	0.471	0.946
(80,60)	1	0.607	0.935	0.496	0.943	0.483	0.946	0.516	0.940	0.475	0.945	0.442	0.948
	2	0.687	0.933	0.515	0.943	0.493	0.946	0.585	0.938	0.484	0.945	0.467	0.947
	3	0.559	0.938	0.479	0.945	0.459	0.948	0.476	0.942	0.445	0.948	0.412	0.950

Table 9. The 95% ACI/HPD estimation results of λ_2.

(n,m)	Design	ACI		HPD				ACI		HPD			
				Group A		Group 2				Group A		Group B	
		AIL	CP	AIL	CP	AIL	CP	AIL	CP	AIL	CP	AIL	CP
		$(T_1,T_2)=(0.5,1.0)$						$(T_1,T_2)=(1.0,1.5)$					
(40,20)	1	1.501	0.921	1.280	0.927	0.936	0.934	1.274	0.930	0.906	0.934	0.816	0.938
	2	1.454	0.923	1.079	0.930	0.871	0.938	1.138	0.934	0.879	0.937	0.782	0.941
	3	1.383	0.926	0.919	0.932	0.769	0.941	1.032	0.936	0.810	0.939	0.752	0.944
(40,30)	1	1.108	0.930	0.805	0.938	0.713	0.941	0.916	0.939	0.761	0.945	0.684	0.947
	2	1.215	0.928	0.841	0.936	0.741	0.941	0.977	0.938	0.786	0.943	0.712	0.944
	3	1.041	0.931	0.786	0.939	0.637	0.944	0.884	0.941	0.729	0.946	0.586	0.949
(80,40)	1	0.970	0.932	0.712	0.941	0.613	0.945	0.824	0.942	0.686	0.947	0.565	0.950
	2	0.842	0.935	0.656	0.942	0.601	0.945	0.715	0.944	0.643	0.949	0.543	0.950
	3	0.806	0.937	0.635	0.943	0.563	0.947	0.684	0.945	0.613	0.950	0.533	0.951
(80,60)	1	0.692	0.942	0.554	0.946	0.511	0.948	0.588	0.950	0.516	0.953	0.486	0.954
	2	0.752	0.939	0.604	0.944	0.524	0.948	0.639	0.947	0.579	0.952	0.514	0.953
	3	0.635	0.943	0.486	0.948	0.468	0.950	0.554	0.951	0.488	0.954	0.436	0.955

Table 10. The 95% ACI/HPD estimation results of σ_1.

(n,m)	Design	ACI		HPD				ACI		HPD			
				Group A		Group 2				Group A		Group B	
		AIL	CP	AIL	CP	AIL	CP	AIL	CP	AIL	CP	AIL	CP
		$(T_1,T_2)=(0.5,1.0)$						$(T_1,T_2)=(1.0,1.5)$					
(40,20)	1	0.763	0.946	0.446	0.963	0.414	0.966	0.625	0.949	0.458	0.965	0.416	0.968
	2	0.830	0.941	0.539	0.957	0.497	0.961	0.749	0.945	0.486	0.961	0.434	0.964
	3	0.783	0.944	0.499	0.961	0.454	0.964	0.811	0.942	0.523	0.958	0.471	0.961
(40,30)	1	0.579	0.954	0.392	0.971	0.353	0.974	0.514	0.955	0.362	0.971	0.339	0.975
	2	0.625	0.951	0.402	0.968	0.388	0.971	0.585	0.952	0.412	0.968	0.383	0.972
	3	0.668	0.950	0.422	0.967	0.394	0.970	0.534	0.953	0.391	0.969	0.364	0.973
(80,40)	1	0.514	0.956	0.357	0.973	0.321	0.975	0.363	0.963	0.337	0.976	0.281	0.979
	2	0.533	0.955	0.367	0.972	0.333	0.975	0.400	0.960	0.347	0.974	0.290	0.977
	3	0.544	0.955	0.374	0.972	0.347	0.975	0.468	0.957	0.355	0.973	0.314	0.976
(80,60)	1	0.412	0.959	0.265	0.976	0.213	0.980	0.297	0.969	0.285	0.979	0.208	0.982
	2	0.443	0.958	0.343	0.975	0.317	0.977	0.346	0.964	0.322	0.977	0.268	0.979
	3	0.433	0.958	0.286	0.975	0.291	0.978	0.313	0.967	0.313	0.977	0.235	0.980

Table 11. The 95% ACI/HPD estimation results of σ_2.

(n,m)	Design	ACI		HPD				ACI		HPD			
				Group A		Group 2				Group A		Group B	
		AIL	CP	AIL	CP	AIL	CP	AIL	CP	AIL	CP	AIL	CP
		$(T_1,T_2)=(0.5,1.0)$						$(T_1,T_2)=(1.0,1.5)$					
(40,20)	1	0.954	0.935	0.815	0.943	0.602	0.949	0.885	0.939	0.806	0.944	0.574	0.951
	2	1.191	0.932	0.932	0.938	0.696	0.944	0.970	0.938	0.823	0.942	0.613	0.948
	3	0.999	0.934	0.859	0.941	0.639	0.947	0.986	0.936	0.914	0.939	0.659	0.946
(40,30)	1	0.825	0.940	0.754	0.946	0.540	0.952	0.791	0.944	0.720	0.949	0.453	0.956
	2	0.874	0.939	0.776	0.945	0.564	0.951	0.830	0.941	0.779	0.946	0.543	0.952
	3	0.919	0.937	0.797	0.944	0.597	0.949	0.819	0.942	0.753	0.947	0.496	0.954
(80,40)	1	0.767	0.943	0.706	0.949	0.500	0.953	0.746	0.946	0.609	0.955	0.313	0.961
	2	0.801	0.941	0.713	0.947	0.513	0.953	0.780	0.945	0.689	0.952	0.345	0.960
	3	0.811	0.941	0.723	0.947	0.533	0.952	0.790	0.944	0.694	0.951	0.414	0.958
(80,60)	1	0.657	0.948	0.583	0.954	0.328	0.960	0.615	0.953	0.516	0.958	0.229	0.964
	2	0.712	0.945	0.681	0.951	0.437	0.956	0.706	0.949	0.575	0.957	0.301	0.962
	3	0.706	0.945	0.623	0.952	0.386	0.958	0.674	0.951	0.547	0.957	0.295	0.962

Table 12. The 95% ACI/HPD estimation results of $S(t)$.

(n,m)	Design	ACI		HPD				ACI		HPD			
				Group A		Group 2				Group A		Group B	
		AIL	CP	AIL	CP	AIL	CP	AIL	CP	AIL	CP	AIL	CP
		$(T_1,T_2)=(0.5,1.0)$						$(T_1,T_2)=(1.0,1.5)$					
(40,20)	1	0.221	0.941	0.144	0.944	0.089	0.950	0.209	0.943	0.132	0.945	0.077	0.952
	2	0.200	0.943	0.126	0.946	0.074	0.954	0.170	0.945	0.111	0.948	0.069	0.954
	3	0.216	0.942	0.134	0.945	0.081	0.951	0.193	0.944	0.125	0.946	0.072	0.952
(40,30)	1	0.194	0.945	0.102	0.948	0.072	0.954	0.168	0.947	0.104	0.950	0.063	0.955
	2	0.158	0.948	0.095	0.953	0.061	0.957	0.147	0.950	0.092	0.954	0.057	0.957
	3	0.186	0.946	0.098	0.951	0.064	0.956	0.154	0.948	0.096	0.953	0.060	0.955
(80,40)	1	0.151	0.948	0.092	0.954	0.059	0.957	0.139	0.950	0.091	0.955	0.055	0.959
	2	0.145	0.949	0.088	0.955	0.050	0.960	0.122	0.951	0.081	0.956	0.047	0.962
	3	0.149	0.949	0.091	0.955	0.054	0.959	0.130	0.951	0.088	0.956	0.051	0.961
(80,60)	1	0.140	0.949	0.085	0.955	0.048	0.960	0.112	0.951	0.078	0.957	0.045	0.962
	2	0.111	0.953	0.066	0.958	0.040	0.961	0.082	0.955	0.063	0.959	0.038	0.964
	3	0.136	0.951	0.079	0.956	0.045	0.961	0.090	0.953	0.072	0.958	0.043	0.963

Table 13. The 95% ACI/HPD estimation results of $h(t)$.

(n,m)	Design	ACI		HPD				ACI		HPD			
				Group A		Group 2				Group A		Group B	
		AIL	CP	AIL	CP	AIL	CP	AIL	CP	AIL	CP	AIL	CP
		$(T_1,T_2)=(0.5,1.0)$						$(T_1,T_2)=(1.0,1.5)$					
(40,20)	1	0.859	0.943	0.698	0.946	0.216	0.956	0.954	0.941	0.735	0.947	0.215	0.955
	2	1.138	0.939	0.770	0.943	0.221	0.953	0.655	0.948	0.524	0.953	0.170	0.961
	3	0.716	0.946	0.584	0.949	0.200	0.959	0.820	0.945	0.646	0.950	0.193	0.958
(40,30)	1	0.685	0.948	0.525	0.951	0.194	0.961	0.539	0.951	0.448	0.955	0.168	0.963
	2	0.629	0.950	0.502	0.953	0.186	0.963	0.485	0.953	0.409	0.957	0.154	0.965
	3	0.611	0.951	0.473	0.954	0.166	0.964	0.462	0.954	0.396	0.958	0.141	0.966
(80,40)	1	0.563	0.955	0.453	0.959	0.149	0.968	0.425	0.957	0.367	0.960	0.125	0.970
	2	0.605	0.952	0.462	0.955	0.151	0.965	0.460	0.954	0.379	0.959	0.134	0.968
	3	0.519	0.957	0.445	0.961	0.145	0.968	0.414	0.959	0.359	0.962	0.122	0.970
(80,60)	1	0.453	0.960	0.437	0.963	0.144	0.969	0.384	0.962	0.330	0.964	0.118	0.971
	2	0.399	0.962	0.382	0.966	0.136	0.971	0.295	0.965	0.274	0.969	0.090	0.972
	3	0.375	0.963	0.282	0.970	0.111	0.973	0.272	0.965	0.214	0.971	0.082	0.973

6. Real competing applications

This section looks at two applications that show how the proposed approaches may be applied in practice, utilizing independent real-world competing risk datasets from the engineering and clinical sectors.

6.1. Electrical appliances

This part investigates an examination of real-world data containing the failure times for electrical appliances that were submitted to an autonomous test using eighteen modes; see Lawless [31]. Following the failures in mode 11, the lifespan of these electrical appliances was assigned to one of three causes: "1" (failure in mode 11) or 2 (failures by other modes). The total number of recorded observations for electrical appliances (reported in Table 14) owing to causes 1 and 2 are 8 and 13, respectively. Later, this set of data has been reanalyzed by Abushal [32]. The failure causes were defined operationally: mode 11 failures were classified as cause 1, while all other modes were grouped as cause 2. This classification was made in a mechanical study, where each device is associated with a single failure cause and time, and the data display does not indicate dependence of failure times.

Table 14. Failure times of electrical appliances.

Time[Cause]										
12[2]	16[2]	16[2]	46[2]	46[2]	52[2]	98[1]	98[2]	270[2]	413[1]	495[1]
495[2]	557[2]	616[2]	692[1]	1065[1]	1107[2]	1193[1]	1467[1]	1467[2]	1937[1]	

Table 15. Fitting the NH model from electrical appliances data.

Cause	Par.	MLE(SE)	95% ACI	$\mathbb{KS}$($\mathbb{P}$-value)
Cause 1	λ_1	0.0020(0.0005)	(0.0011,0.0029)	0.2780(0.4835)
	σ_1	0.7355(0.1781)	(0.3329,1.0311)	
Cause 2	λ_2	0.0241(0.0240)	(0.0007,0.0712)	0.1776(0.8069)
	σ_2	0.3697(0.1364)	(0.1023,0.6370)	

Before evaluating the validity of the proposed estimation results, it is crucial to determine whether the NH distribution provides an appropriate fit for the electrical appliances dataset. For this reason, the goodness-of-fit is examined using the Kolmogorov–Smirnov ($\mathbb{KS}$) test, where both the $\mathbb{KS}$ statistic and its associated significance level ($\mathbb{P}$-value) are evaluated; see Table 15. In Table 15, the MLEs (along with their standard errors (SEs)) and associated 95% ACI bounds for the parameters NH(λ_i, σ_i), $i = 1, 2$, as well as the $\mathbb{KS}$ statistic and its $\mathbb{P}$-value, are obtained. It shows that the null hypothesis, which states that the electrical appliances dataset follows the NH model, cannot be rejected.

To further fitting assessment, graphical representations of the empirical and estimated RF ($R(y)$), probability-probability (PP) plots, and profile log-likelihood curves of λ_i and σ_i (for $i = 1, 2$) are

depicted in Figure 2. These visual diagnostics indicate a strong agreement between the fitted and empirical RF and PP curves for electrical appliance datasets. It also confirms the fitted estimates of $\hat{\lambda}_i$ and $\hat{\sigma}_i$ (for $i = 1, 2$) as presented in Table 15 and demonstrates their existence and uniqueness. Henceforward, we propose adopting the frequentist estimates of λ_i and σ_i (for $i = 1, 2$) as the initial guesses for subsequent computational iterations involving electrical appliances data.

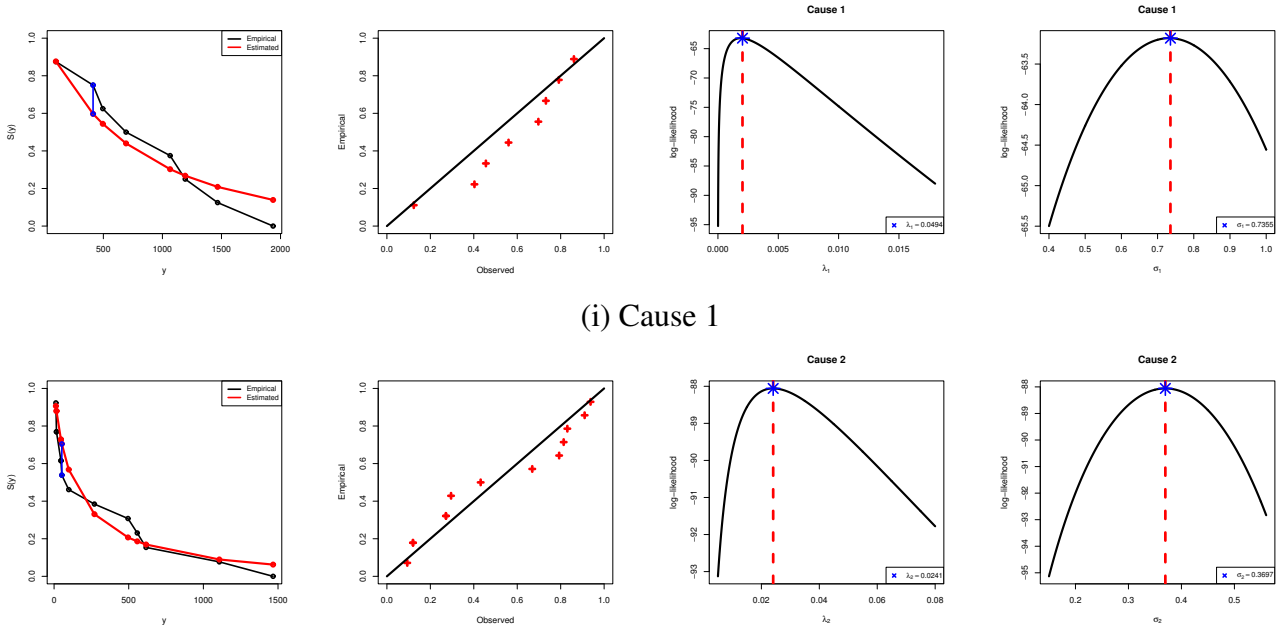

(i) Cause 1

(ii) Cause 2

(a) RF (b) PP (c) Profile of λ (d) Profile of σ

Figure 2. Fitting diagrams of the NH(λ_i, σ_i), $i = 1, 2$ model from electrical appliances data.

Table 16. Several IAPTIIC competing risk samples from electrical appliances data.

Sample	**Q**	$T_1(d_1)$	$T_2(d_2)$	(D_1, D_2)	η	S^*	Time[Cause]				
S1	$(2^5, 0^6)$	50(4)	700(10)	(4,6)	700	3	12[2]	16[2]	46[2]	52[2]	98[1]
							98[2]	270[2]	413[1]	495[1]	692[1]
S2	$(0^3, 2^5, 0^3)$	100(6)	600(9)	(2,7)	600	6	12[2]	16[2]	16[2]	46[2]	52[2]
							98[1]	270[2]	413[1]	557[2]	
S3	$(0^6, 2^5)$	100(7)	300(8)	(1,7)	300	11	12[2]	16[2]	16[2]	46[2]	46[2]
							52[2]	98[1]	270[2]		

In Table 16, three IAPTIIC competing risk samples (with $m = 12$) from electrical appliances data are generated based on different choices of T_i, $i = 1, 2$, and **Q**. Using each Si for $i = 1, 2, 3$, maximum likelihood and Bayesian MCMC estimations with corresponding SEs of λ_i, σ_i (for $i = 1, 2$), $S(t)$, and $h(t)$ (at $t = 50$) are computed; see Table 17. In the same table, two estimated limits of 95% ACI/HPD along with their interval lengths (IL) are computed for λ_i, σ_i (for $i = 1, 2$), $S(t)$, and $h(t)$. In Bayesian

MCMC estimation, assuming the absence of prior knowledge for λ_i and σ_i (for $i = 1, 2$) in the electrical appliances dataset, the hyperparameters (τ_i, κ_i) (of λ_i) and (a_i, b_i) (of σ_i) for $i = 1, 2$, are assigned to be 0.001. Making use of $\mathcal{K} = 12,000$ and $B = 2,000$, the MCMC or 95% HPD intervals estimates of λ_i, σ_i (for $i = 1, 2$), $S(t)$, and $h(t)$ are computed. The results, presented in Table 17, reveal that the Bayesian MCMC estimates of λ_i, σ_i (for $i = 1, 2$), $S(t)$, or $h(t)$ yielded superior performance, exhibiting the lowest SEs and narrowest interval widths. This trend is consistent when comparing asymptotic and credible interval estimates.

Table 17. Estimates of λ_i, σ_i (for $i = 1, 2$), $S(t)$, and $h(t)$ from electrical appliances data.

Sample	Par.	MLE		MCMC		ACI			HPD		
		Est.	St.E	Est.	St.E	Lower	Upper	IL	Lower	Upper	IL
S1	λ_1	0.00002	0.00001	0.00002	0.00010	0.00003	0.00003	0.00003	0.00002	0.00002	0.00004
	λ_2	0.04001	0.04691	0.03824	0.00966	0.00519	0.13194	0.12675	0.01961	0.05658	0.03697
	σ_1	41.3512	5.08890	40.6998	0.35084	30.7375	50.6857	19.9481	40.0093	41.3792	1.36990
	σ_2	0.14379	0.07856	0.14336	0.00995	0.00017	0.29759	0.30794	0.12399	0.16288	0.03890
	$S(t)$	0.81111	0.06802	0.81773	0.02538	0.67780	0.94442	0.26662	0.77115	0.86711	0.09596
	$h(t)$	1.7E-06	1.1E-06	1.6E-06	2.6E-07	0.0E+00	3.7E-06	4.0E-06	1.1E-06	2.1E-06	9.9E-07
S2	λ_1	0.00023	0.00122	0.00022	0.00005	0.00022	0.00261	0.00239	0.00013	0.00031	0.00019
	λ_2	0.05040	0.06028	0.05040	0.00005	0.00068	0.16855	0.16787	0.05030	0.05050	0.00020
	σ_1	1.54881	7.67592	1.51526	0.24761	1.49572	3.5933	2.09750	1.03303	1.99442	0.96139
	σ_2	0.13137	0.06723	0.13137	0.00005	0.00040	0.26313	0.26273	0.13127	0.13146	0.00020
	$S(t)$	0.82076	0.06808	0.82164	0.00377	0.68731	0.95420	0.26689	0.81428	0.82855	0.01427
	$h(t)$	7.9E-07	6.6E-07	7.4E-07	2.1E-07	0.0E+00	2.1E-06	2.6E-06	3.7E-07	1.2E-06	7.8E-07
S3	λ_1	0.00456	0.01864	0.00456	0.00010	0.00032	0.04109	0.04077	0.00436	0.00475	0.00040
	λ_2	0.06318	0.07139	0.06194	0.00992	0.00077	0.20311	0.20234	0.04210	0.08061	0.03850
	σ_1	0.08351	0.24874	0.07901	0.02037	0.00040	0.57104	0.57064	0.04090	0.11852	0.07762
	σ_2	0.12858	0.06389	0.12803	0.00974	0.00336	0.25380	0.25043	0.10890	0.14686	0.03796
	$S(t)$	0.80377	0.07108	0.80815	0.02039	0.66446	0.94307	0.27861	0.76883	0.84669	0.07785
	$h(t)$	7.4E-07	8.7E-07	6.9E-07	1.9E-07	0.0E+00	2.5E-06	3.4E-06	3.2E-07	1.1E-06	7.5E-07

To determine optimal initial values and assess the uniqueness of the fitted estimates of $\hat{\lambda}_i$ and $\hat{\sigma}_i$ (for $i = 1, 2$), the profile log-likelihood functions from Si for $i = 1, 2, 3$ are depicted in Figure 3. It states that the estimated values of $\hat{\lambda}_i$ and $\hat{\sigma}_i$ (for $i = 1, 2$) derived from all Si for $i = 1, 2, 3$, existed and are unique. Consequently, these values are recommended as initial inputs for subsequent numerical procedures.

To assess the behavior of the 40,000 simulated MCMC samples of λ_i, σ_i (for $i = 1, 2$), $S(t)$, and $h(t)$, density plots (by a Gaussian kernel) and trace plots are plotted (using S1 as an example); see Figure 4. In each subplot, the sample mean is represented by a black solid line, while the two bounds of the 95% HPD are marked with black dashed lines. The results demonstrate that the MCMC-generated samples exhibit adequate mixing, ensuring proper convergence. Moreover, the estimated marginal densities of λ_i, σ_i (for $i = 1, 2$), $S(t)$, or $h(t)$ are observed to be approximately symmetric, supporting the validity of the posterior distributions. Furthermore, the chosen burn-in period is sufficiently large to mitigate the influence of initial parameter values, thereby facilitating an efficient and well-mixed sample collection.

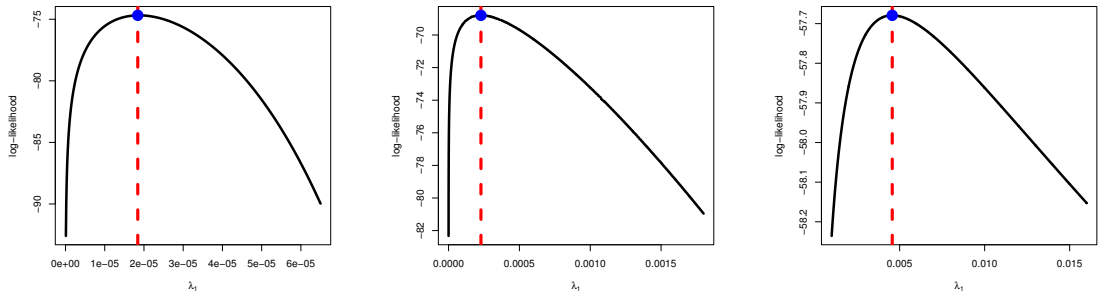

(i) λ_1

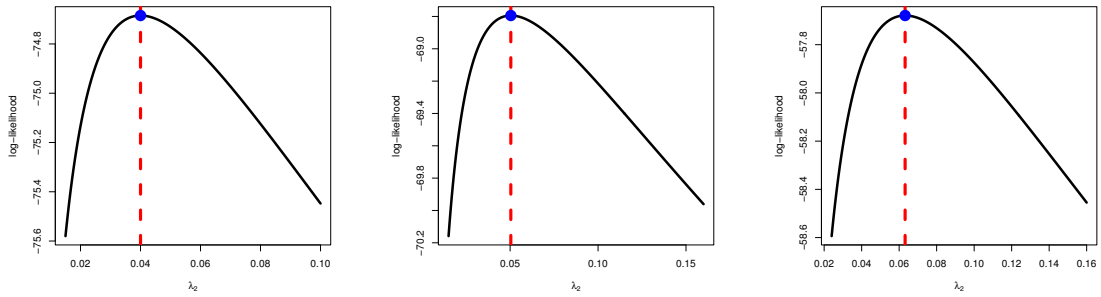

(ii) λ_2

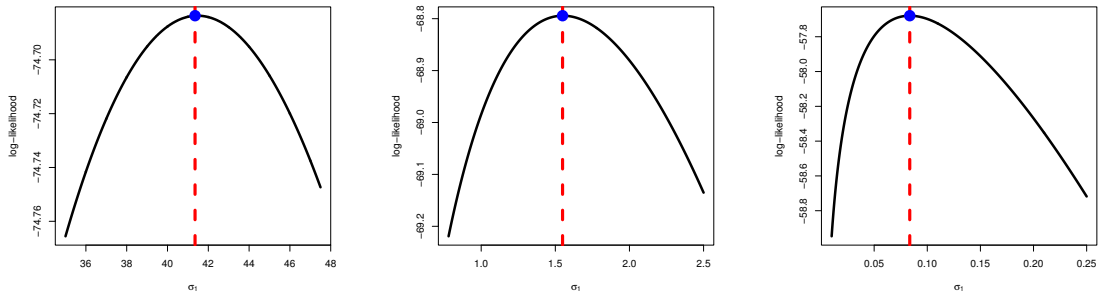

(iii) σ_1

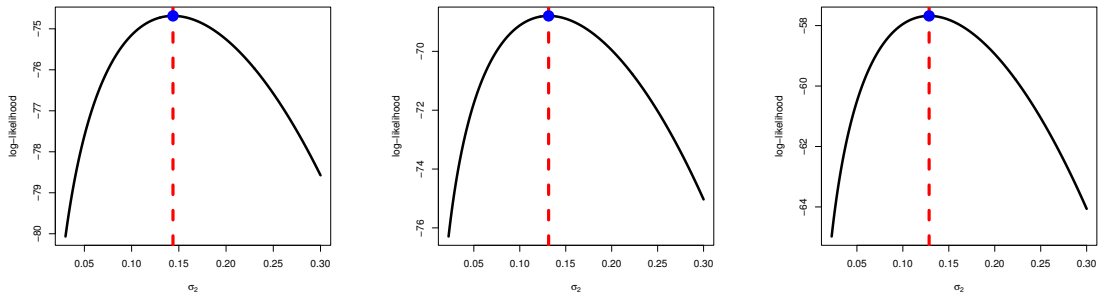

(iv) σ_2

(a) Sample S1 (b) Sample S2 (c) Sample S3

Figure 3. Profile log-likelihoods for λ_i and σ_i (for $i = 1, 2$) from electrical appliances data.

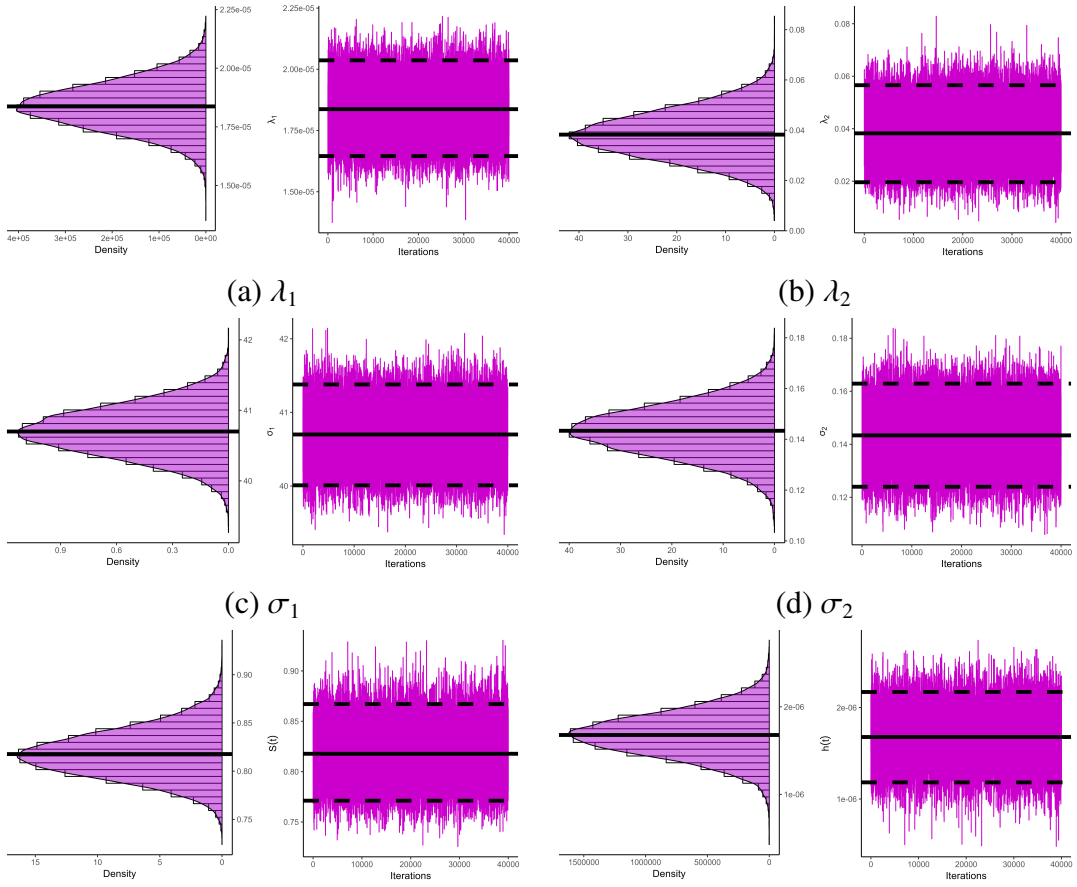

(a) λ_1 (b) λ_2

(c) σ_1 (d) σ_2

(e) $S(t)$ (f) $h(t)$

Figure 4. MCMC plots of λ_i, σ_i (for $i = 1, 2$), $S(t)$, and $h(t)$ from electrical appliances data.

6.2. Multiple myeloma

This example focuses on the analysis of a clinical dataset consisting of observations from 35 patients diagnosed with multiple myeloma. Among these cases, 19 patients experienced disease relapse, while 10 cases were attributed to transplant-related mortality, which serves as a competing risk; see Donoghoe and Gebski [33]. The patients received treatment at the Clinic for Stem Cell Transplantation, University Hospital Hamburg-Eppendorf, Hamburg, Germany.

To investigate the influence of donor haplotypes on relapse time, a proportional sub-distribution hazards model was employed. This model utilizes transplant recipient data categorized based on donor haplotypes: type 'AA' versus type 'AB' or 'BB'. The model specifically quantifies the extended time to relapse associated with donors carrying category 'B' killer immunoglobulin-like receptor haplotypes. For analytical purposes, relapse events are designated as cause 1, while transplant-related mortality is classified as cause 2; see Table 18. Further methodological details can be found in Nassar et al. [34].

Following the same fitting scenarios discussed in Subsection 6.1, Table 19 and Figure 5 evaluate whether the Weibull distribution can provide an acceptable fit or not to multiple myeloma datasets. The fitting outcomes reported in Table 19 indicate that the proposed entire multiple myeloma datasets follow the NH distribution satisfactorily. This fact has also been supported by Figure 5, which reveals

that the fitted RFs match the corresponding empirical RFs for both multiple myeloma datasets. Additionally, it also shows that the fitted values of $\hat{\lambda}_i,\ i = 1, 2$ and $\hat{\sigma}_i,\ i = 1, 2$ (reported in Table 19) exist and are unique.

Table 18. Multiple myeloma dataset.

Time[Cause]									
0.26[2]	0.66[2]	1.81[2]	1.94[2]	1.97[2]	3.45[1]	3.55[2]	3.58[1]	3.81[1]	3.91[2]
4.14[1]	4.57[1]	5.03[1]	6.21[2]	6.70[2]	9.33[1]	9.92[1]	10.68[1]	12.35[1]	14.72[1]
14.82[2]	15.74[1]	17.31[1]	22.31[1]	28.29[1]	41.17[1]	41.17[1]	45.96[1]	80.46[1]	

Table 19. Fitting the NH model from myeloma data.

Cause	Par.	MLE(SE)	95% ACI	$\mathbb{KS}(\mathbb{P}$-value)
Cause 1	λ_1	0.0494(0.0430)	(0.0000,0.1336)	0.1594(0.7197)
	σ_1	1.0184(0.5412)	(0.0000,2.0792)	
Cause 2	λ_2	0.2233(0.2795)	(0.0000,0.7711)	0.1465(0.9621)
	σ_2	1.0443(0.8058)	(0.0000,2.6236)	

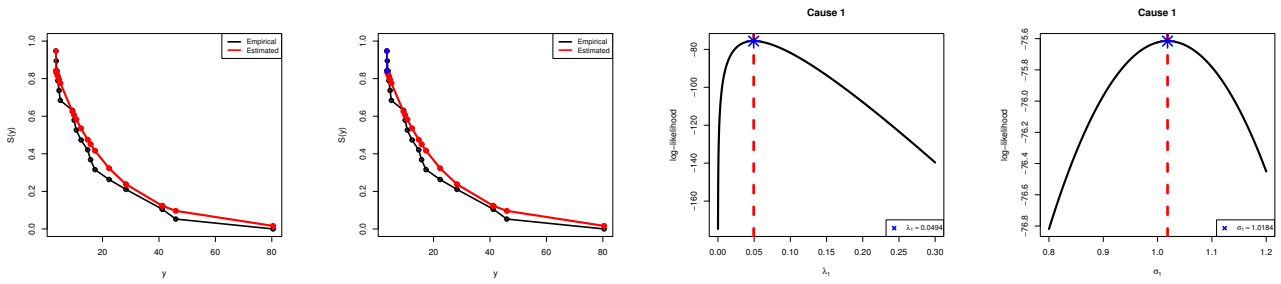

(i) Cause 1

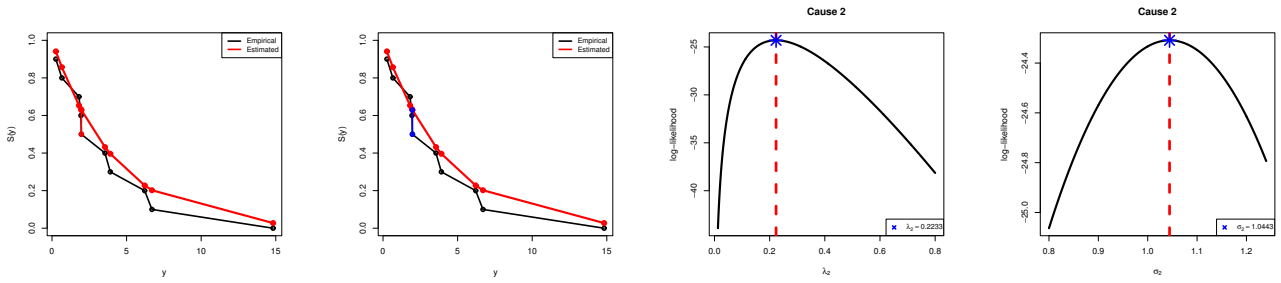

(ii) Cause 2

(a) RF (b) PP (c) Profile of λ (d) Profile of σ

Figure 5. Fitting diagrams of the NH$(\lambda_i, \sigma_i),\ i = 1, 2$ model from myeloma data.

Table 20. Several IAPTIIC competing risk samples from myeloma data.

Sample	**Q**	$T_1(d_1)$	$T_2(d_2)$	(D_1, D_2)	η	S^*	Time[Cause]				
S1	$(2^7, 0^8)$	4(5)	15(14)	(7,7)	15	5	0.26[2]	1.81[2]	1.94[2]	3.55[2]	3.91[2]
							4.14[1]	4.57[1]	5.03[1]	6.70[2]	9.33[1]
							9.92[1]	10.68[1]	12.35[1]	14.82[2]	
S2	$(0^4, 2^7, 0^4)$	3.6(7)	10(12)	(5,7)	10	11	0.26[2]	0.66[2]	1.81[2]	1.94[2]	1.97[2]
							3.55[2]	3.58[1]	3.81[1]	4.14[1]	5.03[1]
							6.21[2]	9.33[1]			
S3	$(0^8, 2^7)$	4(9)	5(10)	(4,6)	5	17	0.26[2]	0.66[2]	1.81[2]	1.94[2]	1.97[2]
							[1]	3.55[2]	[1]	3.81[1]	4.57[1]

Now, for specified $m = 15$ and different options of **Q** and T_i, $i = 1, 2$, three different IAPTIIC competing risk samples under different choices of T_i, $i = 1, 2$ are generated; see Table 20. In Table 21, based on each dataset in Table 20, the proposed point estimates and respective interval estimates of the unknown NH competing risk parameters λ_i and σ_i (for $i = 1, 2$) and of the reliability operators $S(t)$ and $h(t)$ at distinct time $t = 2$ are calculated. Table 21 shows that, in terms of minimal SE and IL values, the Bayesian point and 95% HPD interval estimates outperform those derived using the likelihood setup. All Bayes evaluations developed from myeloma data are done using the same Bayes setups discussed from electrical appliances data (in Subsection 6.1). Profile log-likelihood curves (depicted in Figure 7), based on all created samples Si for $i = 1, 2, 3$, are unimodal and show that the MLEs of them are close to their frequentist estimates listed in Table 21. Figure 6, from S1 as an example, shows that the obtained 40,000 MCMC variates of λ_i, σ_i (for $i = 1, 2$), $S(t)$, or $h(t)$ converge well, and their simulated marginal density estimates behave largely symmetrically.

The two predefined thresholds, T_1 and T_2, play an important role in estimating any parametric function of unknown parameters. Thus, the results gathered from the electrical appliances or myeloma dataset provide a good overview of the NH competing risks model. It should be noted that the proposed estimates calculated here will not be sufficient to determine which statistical approach provides better estimates, because we do not know the actual values of the unknown parameters.

The comprehensive applications analysis demonstrates the practical utility of the proposed methods by applying them to independent, real-world competing risk datasets drawn from both engineering and clinical domains, specifically involving electrical appliances and multiple myeloma cases. Through the findings of these applications, the effectiveness and adaptability of the proposed approaches in addressing complex, real-life reliability challenges are validated. The estimated parameters of the NH competing risks model provide meaningful insights into the failure process, with scale and shape parameters reflecting the intensity and variability of failures from each cause. The presented analysis revealed that certain causes dominate the failure mechanism, which is crucial for understanding and improving system reliability. The inclusion of an improved adaptive censoring scheme further enhanced estimation accuracy, especially under complex or incomplete data scenarios. Overall, the proposed method demonstrates strong practical value and flexibility in modeling competing risks data from real-world applications.

Table 21. Estimates of λ_i, σ_i (for $i = 1, 2$), $S(t)$, and $h(t)$ from myeloma data.

Sample	Par.	MLE		MCMC		ACI			HPD		
		Est.	St.E	Est.	St.E	Lower	Upper	IL	Lower	Upper	IL
S1	λ_1	0.00037	0.00011	0.00037	0.00001	0.00025	0.00060	0.00045	0.00035	0.00039	0.00004
	λ_2	0.60941	0.87440	0.60923	0.01001	0.00438	2.32320	2.31884	0.58946	0.62854	0.03908
	σ_1	103.864	7.07589	103.811	0.75752	89.9960	117.733	27.7370	102.321	105.278	2.95715
	σ_2	0.17190	0.12230	0.17144	0.00998	0.00678	0.41160	0.40479	0.15215	0.19111	0.03896
	$S(t)$	0.79640	0.06637	0.79685	0.00762	0.66631	0.92649	0.26018	0.78193	0.81167	0.02974
	$h(t)$	0.00227	0.00117	0.00226	0.00017	0.00002	0.00457	0.00455	0.00195	0.00260	0.00065
S2	λ_1	0.00067	0.00040	0.00067	0.00001	0.00012	0.00146	0.00138	0.00065	0.00069	0.00004
	λ_2	0.70343	0.97077	0.70326	0.00995	0.01992	2.60610	2.58620	0.68444	0.72342	0.03898
	σ_1	40.0371	17.8417	39.9665	0.75351	5.06806	75.0062	69.9381	38.5069	41.4512	2.94432
	σ_2	0.14238	0.10340	0.14181	0.00977	0.00028	0.34504	0.34471	0.12301	0.16126	0.03825
	$S(t)$	0.82829	0.05410	0.82887	0.00821	0.72225	0.93432	0.21207	0.81260	0.84469	0.03209
	$h(t)$	0.00134	0.00076	0.00133	0.00011	0.00015	0.00282	0.00267	0.00111	0.00154	0.00042
S3	λ_1	0.00064	0.00032	0.00064	0.00001	0.00002	0.00126	0.00124	0.00062	0.00066	0.00004
	λ_2	0.57752	1.00049	0.57731	0.00995	0.01383	2.53845	2.52470	0.55851	0.59752	0.03901
	σ_1	51.3575	9.04009	51.2905	0.75327	33.6392	69.0757	35.4365	49.8272	52.7715	2.94435
	σ_2	0.15951	0.16537	0.15898	0.00983	0.00165	0.48362	0.48200	0.13965	0.17817	0.03852
	$S(t)$	0.82028	0.05670	0.82077	0.00724	0.70915	0.93141	0.22227	0.80663	0.83493	0.02829
	$h(t)$	0.00169	0.00111	0.00168	0.00012	0.00049	0.00388	0.00344	0.00144	0.00193	0.00048

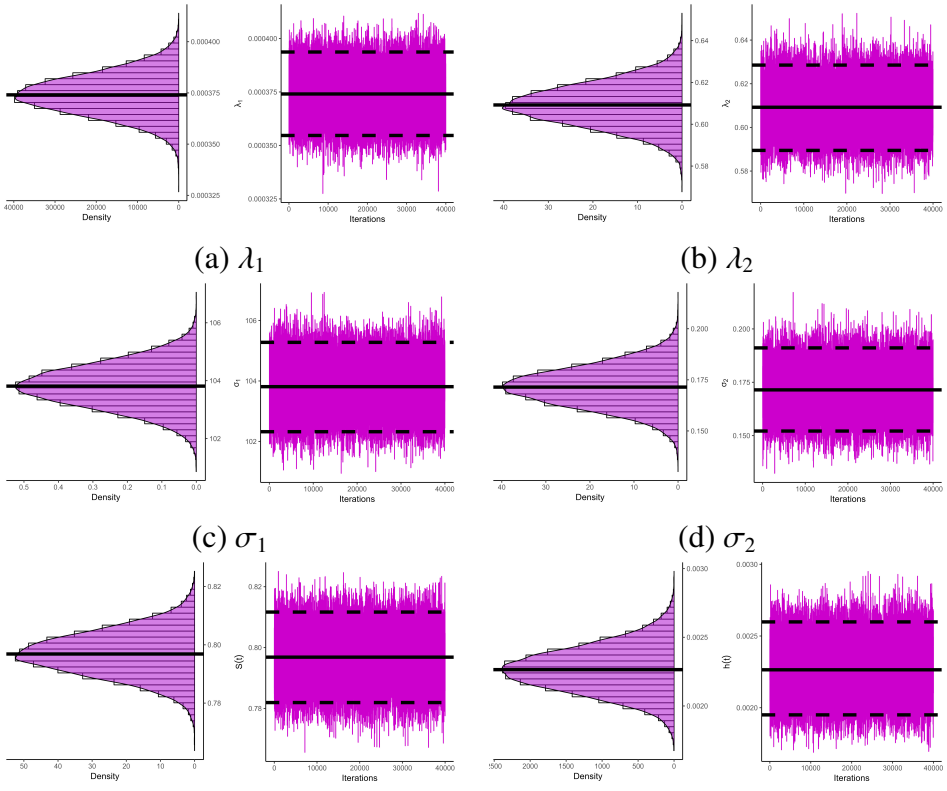

(a) λ_1 (b) λ_2

(c) σ_1 (d) σ_2

(e) $S(t)$ (f) $h(t)$

Figure 6. MCMC plots of λ_i, σ_i (for $i = 1, 2$), $S(t)$, and $h(t)$ from myeloma data.

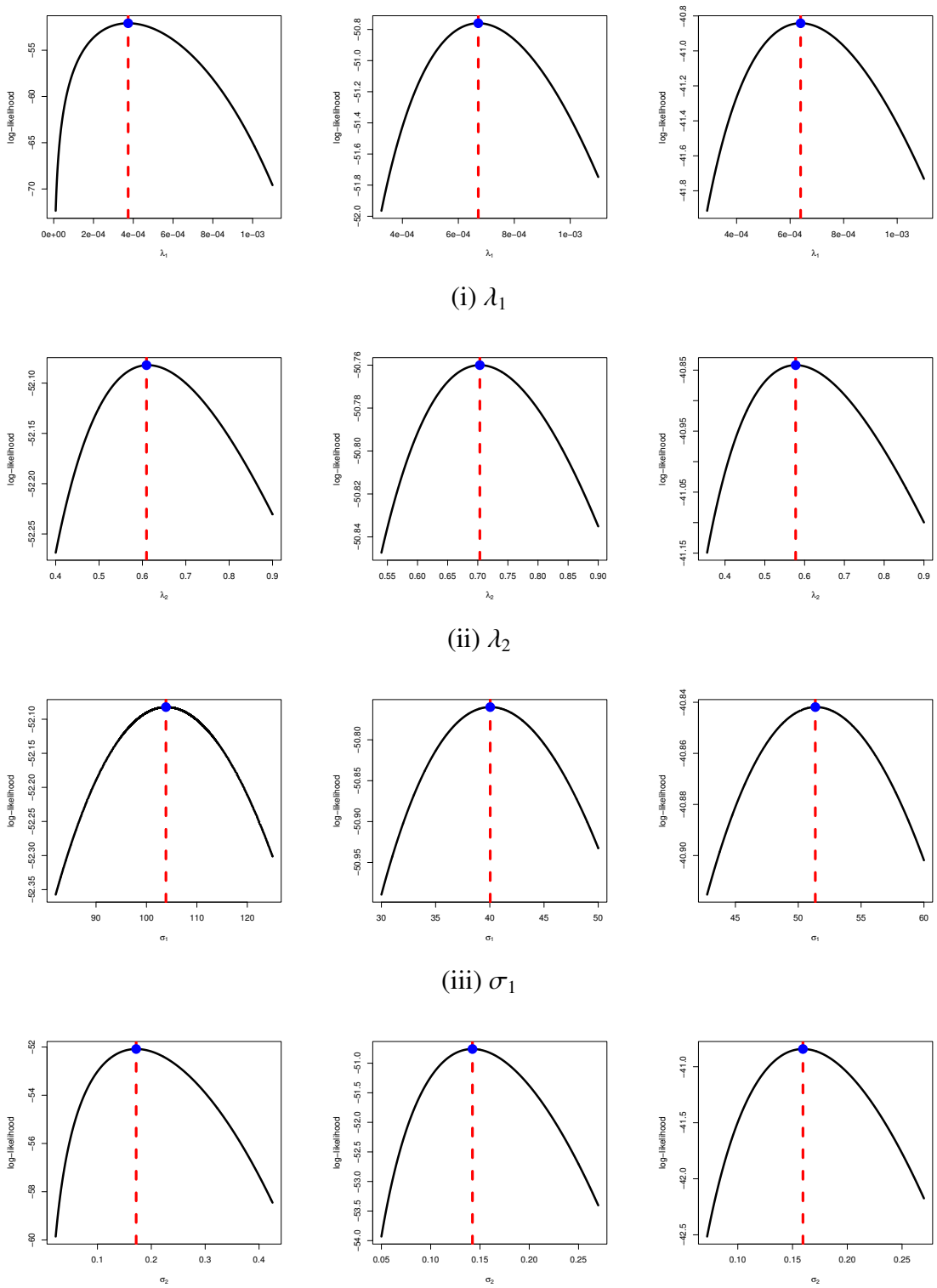

(i) λ_1

(ii) λ_2

(iii) σ_1

(iv) σ_2

(a) Sample S1 (b) Sample S2 (c) Sample S3

Figure 7. Profile log-likelihoods for λ_i and σ_i (for $i = 1, 2$) from myeloma data.

7. Concluding remarks

This research established a comprehensive statistical framework for analyzing the NH competing risks model under an improved adaptive progressively Type-II censored scheme. Various point estimations of model parameters, reliability/survival, and failure rate functions were explored using maximum likelihood and Bayesian estimation methods with independent gamma priors. Additionally, approximate confidence intervals and highest posterior density credible intervals were constructed. Monte Carlo simulations were conducted across different parameter configurations, censoring schemes, and time thresholds. From an applied perspective, two real-world competing risks datasets were analyzed, demonstrating the model's flexibility in capturing diverse failure patterns. The integration of the NH distribution within a competing risks framework enhanced its adaptability for various reliability studies. Meanwhile, the improved adaptive progressive Type-II censoring scheme efficiently balanced the need for timely experimental conclusions with adequate failure data collection, particularly benefiting the assessment of highly reliable products. A comparative analysis of frequentist and Bayesian estimation approaches showed that both methods performed well, with precision improving as sample size increased. When evaluating the performance of different censoring scenarios $Q_i,\ i = 1, 2, \ldots, m$, it reveals that: (i) all estimates of $\sigma_i,\ i = 1, 2$ achieve optimal performance when left censoring occurs; (ii) all estimates of $\lambda_i,\ i = 1, 2$ and $h(t)$ achieve optimal performance when right censoring occurs; and (iii) all estimates of $S(t)$ achieve optimal performance when middle censoring occurs. The Bayesian approach, utilizing informative priors, proved especially advantageous for small-sample scenarios, yielding more stable estimates. Analysis of two real-world datasets representing electrical device failures or multiple myeloma demonstrated how the NH competing risks model effectively captured multi-cause failure data, enabling more accurate reliability assessments than traditional single-cause models. While the independent assumption between the latent failure times significantly simplifies the derivation of the likelihood function and facilitates parameter estimation, it is indeed a strong condition that may not hold in many practical applications. For instance, if the failure mechanisms are influenced by shared environmental stressors or unobserved heterogeneity, the independence assumption may lead to biased estimates of reliability characteristics. See, for more details, Moeschberger and Klein [35], Du and Gui [36], and Michimae [37]. Extending the current framework to accommodate dependent competing risks represents a natural and valuable direction for future research. One promising approach involves modeling the joint distribution using copula functions, which allow for flexible dependence structures while preserving the interpretability of marginal distributions. Such approaches would further enhance the applicability of the NH competing risks model in complex reliability systems.

Author contributions

Refah Alotaibi: Conceptualization, Methodology, Investigation, Funding acquisition, Writing – original draft; Mazen Nassar: Conceptualization, Methodology, Investigation, Writing – review & editing; Ahmed Elshahhat: Software, Data curation, Writing – original draft. All authors have read and agreed to the published version of the manuscript.

Use of Generative-AI tools declaration

The authors declare that they have not used Artificial Intelligence (AI) tools in the creation of this article.

Funding

This research was funded by Princess Nourah bint Abdulrahman University Researchers Supporting Project number (PNURSP2025R50), Princess Nourah bint Abdulrahman University, Riyadh, Saudi Arabia.

Data Availability

The authors confirm that the data supporting the findings of this study are available within the article.

Conflicts of Interest

The authors declare no conflict of interest.

References

1. D. R. Cox, The analysis of exponentially distributed life-times with two types of failure, *J. Roy. Stat. Soc. Ser. B: Stat. Methodol.*, **21** (1959), 411–421. http://doi.org/10.1111/j.2517-6161.1959.tb00349.x
2. E. Cramer, A. B. Schmiedt, Progressively Type-II censored competing risks data from Lomax distributions, *Comput. Stat. Data Anal.*, **55** (2011), 1285–1303. http://doi.org/10.1016/j.csda.2010.09.017
3. E. A. Ahmed, Z. Ali Alhussain, M. M. Salah, H. Haj Ahmed, M. S. Eliwa, Inference of progressively type-II censored competing risks data from Chen distribution with an application, *J. Appl. Stat.*, **47** (2020), 2492–2524. http://doi.org/10.1080/02664763.2020.1815670
4. T. A. Abushal, J. Kumar, A. H. Muse, A. H. Tolba, Estimation for Akshaya failure model with competing risks under progressive censoring scheme with analyzing of thymic lymphoma of mice application, *Complexity*, **2022** (2022), 5151274. http://doi.org/10.1155/2022/5151274
5. M. A. Almuqrin, M. M. Salah, E. A. Ahmed, Statistical inference for competing risks model with adaptive progressively type-II censored Gompertz life data using industrial and medical applications, *Mathematics*, **10** (2022), 4274. http://doi.org/10.3390/math10224274
6. Y. Tian, Y. Liang, W. Gui, Inference and optimal censoring scheme for a competing-risks model with type-II progressive censoring, *Math. Popul. Stud.*, **31** (2024), 1–39. http://doi.org/10.1080/08898480.2023.2225349

7. R. Alotaibi, M. Nassar, Z. A. Khan, W. A. Alajlan, A. Elshahhat, Analysis and data modelling of electrical appliances and radiation dose from an adaptive progressive censored XGamma competing risk model, *J. Radiat. Res. Appl. Sci.*, **18** (2025), 101188. http://doi.org/10.1016/j.jrras.2024.101188
8. S. Han, D. Wang, Y. A. Tashkandy, M. E. Bakr, M. M. M. El-Din, A. Elshenawya, A new sine-inspired probability model: Theoretical features with statistical modeling of the music engineering and reliability scenarios, *Alexandria Eng. J.*, **106** (2024), 288–297. http://doi.org/10.1016/j.aej.2024.06.099
9. A. Haddari, H. Zeghdoudi, R. Pakyari, A new two-parameter family of discrete distributions, *Heliyon*, **11** (2025), e41459. http://doi.org/10.1016/j.heliyon.2024.e41459
10. M. Kouadria, H. Zeghdoudi, The truncated new-XLindley distribution with applications, *J. Comput. Anal. Appl.*, **34** (2025), 53–64.
11. C. S. Kumar, G. Jithu, V. Deneshkumar, S. N. Chandra, On alpha generalized Kies model and its applications in cancer data sets, *Jpn. J. Stat. Data Sci.*, **8** (2025), 539–557. http://doi.org/10.1007/s42081-024-00284-9
12. S. Nadarajah, F. Haghighi, An extension of the exponential distribution, *Statistics*, **45** (2011), 543–558. http://doi.org/10.1080/02331881003678678
13. M. Wu, W. Gui, Estimation and prediction for Nadarajah-Haghighi distribution under progressive type-II censoring, *Symmetry*, **13** (2021), 999. http://doi.org/10.3390/sym13060999
14. S. Dey, L. Wang, M. Nassar, Inference on Nadarajah-Haghighi distribution with constant stress partially accelerated life tests under progressive type-II censoring, *J. Appl. Stat.*, **49** (2022), 2891–2912. http://doi.org/10.1080/02664763.2021.1928014
15. I. Elbatal, N. Alotaibi, S. A. Alyami, M. Elgarhy, A. R. El-Saeed, Bayesian and non-Bayesian estimation of the Nadaraj ah-Haghighi distribution: Using progressive Type-1 censoring scheme, *Mathematics*, **10** (2022), 760. http://doi.org/10.3390/math10050760
16. A. M. Almarashi, A. Algarni, H. Okasha, M. Nassar, On reliability estimation of Nadarajah-Haghighi distribution under adaptive type-I progressive hybrid censoring scheme, *Qual. Reliab. Eng. Int.*, **38** (2022), 817–833. http://doi.org/10.1002/qre.3016
17. T. A. Abushal, Statistical inference for Nadarajah-Haghighi distribution under unified hybrid censored competing risks data, *Heliyon*, **10** (2024), e26794. http://doi.org/10.1016/j.heliyon.2024.e26794
18. M. E. Abd Elwahab, A. Elshahhat, O. A. Alqasem, M. Nassar, Reliability analysis of new jointly type-II hybrid NH censored data and its modeling for three engineering cases, *Alexandria Eng. J.*, **113** (2025), 347–365. http://doi.org/10.1016/j.aej.2024.11.032
19. N. Balakrishnan, D. Kundu, Hybrid censoring: Models, inferential results and applications, *Comput. Stat. Data Anal.*, **57** (2013), 166–209. http://doi.org/10.1016/j.csda.2012.03.025
20. N. Balakrishnan, N. Kannan, C. T. Lin, S. J. S. Wu, Inference for the extreme value distribution under progressive Type-II censoring, *J. Stat. Comput. Simul.*, **74** (2004), 25–45. http://doi.org/10.1080/0094965031000105881

21. M. K. Rastogi, Y. M. Tripathi, Estimating the parameters of a Burr distribution under progressive type II censoring, *Stat. Method.*, **9** (2012), 381–391. http://doi.org/10.1016/j.stamet.2011.10.002

22. O. E. Abo-Kasem, A. R. El Saeed, A. I. El Sayed, Optimal sampling and statistical inferences for Kumaraswamy distribution under progressive Type-II censoring schemes, *Sci. Rep.*, **13** (2023), 12063. http://doi.org/10.1038/s41598-023-38594-9

23. M. M. Hasaballah, Y. A. Tashkandy, M. E. Bakr, O. S. Balogun, D. A. Ramadan, Classical and Bayesian inference of inverted modified Lindley distribution based on progressive type-II censoring for modeling engineering data, *AIP Adv.*, **14** (2024). http://doi.org/10.1063/5.0190542

24. H. K. T. Ng, D. Kundu, P. S. Chan, Statistical analysis of exponential lifetimes under an adaptive Type-II progressive censoring scheme, *Nav. Res. Log.*, **56** (2009), 687–698. http://doi.org/10.1002/nav.20371

25. M. M. A. Sobhi, A. A. Soliman, Estimation for the exponentiated Weibull model with adaptive Type-II progressive censored schemes, *Appl. Math. Modell.*, **40** (2016), 1180–1192. http://doi.org/10.1016/j.apm.2015.06.022

26. H. Panahi, N. Moradi, Estimation of the inverted exponentiated Rayleigh distribution based on adaptive Type II progressive hybrid censored sample, *J. Comput. Appl. Math.*, **364** (2020), 112345. http://doi.org/10.1016/j.cam.2019.112345

27. S. Dutta, S. Dey, S. Kayal, Bayesian survival analysis of logistic exponential distribution for adaptive progressive Type-II censored data, *Comput. Stat.*, **39** (2024), 2109–2155. http://doi.org/10.1007/s00180-023-01376-y

28. W. Yan, P. Li, Y. Yu, Statistical inference for the reliability of Burr-XII distribution under improved adaptive Type-II progressive censoring, *Appl. Math. Modell.*, **95** (2021), 38–52. http://doi.org/10.1016/j.apm.2021.01.050

29. A. Henningsen, O. Toomet, maxLik: A package for maximum likelihood estimation in R, *Comput. Stat.*, **26** (2011), 443–458. http://doi.org/10.1007/s00180-010-0217-1

30. M. Plummer, N. Best, K. Cowles, K. Vines, CODA: Convergence diagnosis and output analysis for MCMC, *R News*, **6** (2006), 7–11.

31. J. F. Lawless, *Statistical Models and Methods For Lifetime Data*, 2 Eds., New Jersey: John Wiley and Sons, 2011.

32. T. A. Abushal, Statistical inference for Nadarajah-Haghighi distribution under unified hybrid censored competing risks data, *Heliyon*, **10** (2024), e26794. http://doi.org/10.1016/j.heliyon.2024.e26794

33. M. W. Donoghoe, V. Gebski, The importance of censoring in competing risks analysis of the subdistribution hazard, *BMC Med. Res. Method.*, **17** (2017), 52. http://doi.org/10.1186/s12874-017-0327-3

34. M. Nassar, R. Alotaibi, C. Zhang, Estimation of reliability indices for alpha power exponential distribution based on progressively censored competing risks data, *Mathematics*, **10** (2022), 2258. http://doi.org/10.3390/math10132258

35. M. L. Moeschberger, J. P. Klein, Statistical methods for dependent competing risks, *Lifetime Data Anal.*, **1** (1995), 195–204. http://doi.org/10.1007/BF00985770

36. Y. Du, W. Gui, Statistical inference of adaptive type II progressive hybrid censored data with dependent competing risks under bivariate exponential distribution, *J. Appl. Stat.*, **49** (2022), 3120–3140. http://doi.org/10.1080/02664763.2021.1937961

37. H. Michimae, T. Emura, A. Miyamoto, K. Kishi, Bayesian parametric estimation based on left-truncated competing risks data under bivariate Clayton copula models, *J. Appl. Stat.*, **51** (2024), 2690–2708. http://doi.org/10.1080/02664763.2024.2315458

Appendix

Appendix A

The normal equations obtained from the log-likelihood function in (3.2) are as follows:

$$\begin{aligned}\frac{\partial \ell(\boldsymbol{\Theta}|\underline{\mathbf{y}})}{\partial \lambda_1} &= \frac{D_1}{\lambda_1} + (\sigma_1 - 1)\sum_{i=1}^{D_1}\frac{y_i}{\omega(y_i;\lambda_1)} - \sigma_1\sum_{i=1}^{D} y_i[\omega(y_i;\lambda_1)]^{\sigma_1-1} - \sigma_1\sum_{i=1}^{J} y_i Q_i[\omega(y_i;\lambda_1)]^{\sigma_1-1} \\ &- \sigma_1\eta S^*[\omega(\eta;\lambda_1)]^{\sigma_1-1} = 0,\end{aligned}$$

$$\begin{aligned}\frac{\partial \ell(\boldsymbol{\Theta}|\underline{\mathbf{y}})}{\partial \lambda_2} &= \frac{D_2}{\lambda_2} + (\sigma_2 - 1)\sum_{i=1}^{D_2}\frac{y_i}{\omega(y_i;\lambda_2)} - \sigma_2\sum_{i=1}^{D} y_i[\omega(y_i;\lambda_2)]^{\sigma_2-1} - \sigma_2\sum_{i=1}^{J} y_i Q_i[\omega(y_i;\lambda_2)]^{\sigma_2-1} \\ &- \sigma_2\eta S^*[\omega(\eta;\lambda_2)]^{\sigma_2-1} = 0,\end{aligned}$$

$$\begin{aligned}\frac{\partial \ell(\boldsymbol{\Theta}|\underline{\mathbf{y}})}{\partial \sigma_1} &= \frac{D_1}{\sigma_1} + \sum_{i=1}^{D_1}\log[\omega(y_i;\lambda_1)] - \sum_{i=1}^{D}[\omega(y_i;\lambda_1)]^{\sigma_1}\log[\omega(y_i;\lambda_1)] \\ &- \sum_{i=1}^{J} Q_i[\omega(y_i;\lambda_1)]^{\sigma_1}\log[\omega(y_i;\lambda_1)] - S^*[\omega(\eta;\lambda_1)]^{\sigma_1}\log[\omega(\eta;\lambda_1)] = 0\end{aligned}$$

and

$$\begin{aligned}\frac{\partial \ell(\boldsymbol{\Theta}|\underline{\mathbf{y}})}{\partial \sigma_2} &= \frac{D_2}{\sigma_2} + \sum_{i=1}^{D_2}\log[\omega(y_i;\lambda_2)] - \sum_{i=1}^{D}[\omega(y_i;\lambda_2)]^{\sigma_2}\log[\omega(y_i;\lambda_2)] \\ &- \sum_{i=1}^{J} Q_i[\omega(y_i;\lambda_2)]^{\sigma_2}\log[\omega(y_i;\lambda_2)] - S^*[\omega(\eta;\lambda_2)]^{\sigma_2}\log[\omega(\eta;\lambda_2)] = 0.\end{aligned}$$

Appendix B

The second-order partial derivatives of the log-likelihood function in (3.2) are as follows:

$$\begin{aligned}\frac{\partial^2 \ell(\boldsymbol{\Theta}|\underline{\mathbf{y}})}{\partial \lambda_c^2} &= -\frac{D_c}{\lambda_c^2} - (\sigma_c - 1)\sum_{i=1}^{D_c}\frac{y_i^2}{[\omega(y_i;\lambda_c)]^2} - \sigma_c(\sigma_c - 1)\sum_{i=1}^{D} y_i^2[\omega(y_i;\lambda_c)]^{\sigma_c-2} \\ &- \sigma_c(\sigma_c - 1)\sum_{i=1}^{J} Q_i y_i^2[\omega(y_i;\lambda_c)]^{\sigma_c-2} - \sigma_c(\sigma_c - 1)S^*\eta^2[\omega(\eta;\lambda_c)]^{\sigma_c-2},\end{aligned}$$

$$\frac{\partial^2 \ell(\boldsymbol{\Theta}|\underline{\mathbf{y}})}{\partial \sigma_c^2} = -\frac{D_c}{\sigma_c^2} - \sum_{i=1}^{D} \omega(y_i;\lambda_c)^{\sigma_c}[\log \omega(y_i;\lambda_c)]^2 - \sum_{i=1}^{J} Q_i \omega(y_i;\lambda_c)^{\sigma_c}[\log \omega(y_i;\lambda_c)]^2 - S^* \omega(\eta;\lambda_c)^{\sigma_c}[\log \omega(\eta;\lambda_c)]^2$$

and

$$\frac{\partial^2 \ell(\boldsymbol{\Theta}|\underline{\mathbf{y}})}{\partial \lambda_c \partial \sigma_c} = \sum_{i=1}^{D_c} \frac{y_i}{\omega(y_i;\lambda_c)} - \sum_{i=1}^{D} y_i \omega(y_i;\lambda_c)^{\sigma_c - 1}[1 + \sigma_c \log \omega(y_i;\lambda_c)] - \sum_{i=1}^{J} Q_i y_i \omega(y_i;\lambda_c)^{\sigma_c - 1}[1 + \sigma_c \log \omega(y_i;\lambda_c)] - S^* \eta \omega(\eta;\lambda_c)^{\sigma_c - 1}[1 + \sigma_c \log \omega(\eta;\lambda_c)].$$

AIMS Press